Copy

CONFIDENTIAL

62 72157 606

NASA TM X-333

NASA TM X-333

CLASSIFICATION CHANGED
UNCLASSIFIED
To
By Authority of T-D 71-67 Date 10/5/71

TECHNICAL MEMORANDUM

X-333

LOW-SPEED INVESTIGATION OF THE EFFECTS OF WING FLAP DEFLECTION AND HORIZONTAL-TAIL CONFIGURATION ON THE LONGITUDINAL AERODYNAMIC CHARACTERISTICS OF AN AIRPLANE CONFIGURATION HAVING TAIL SURFACES OUTBOARD OF THE WING TIPS

By William C. Hayes, Jr., and William C. Sleeman, Jr.

Langley Research Center
Langley Field, Va.

Declassified by authority of NASA Classification Change Notices No. 215
Dated ** 12/31/71

N71-75279
(ACCESSION NUMBER)
37
(PAGES)
(NASA CR OR TMX OR AD NUMBER)
(THRU)
None
(CODE)
(CATEGORY)
FACILITY FORM 602

NATIONAL AERONAUTICS AND SPACE ADMINISTRATION
WASHINGTON
September 1960

CONFIDENTIAL

1K

[redacted]

NATIONAL AERONAUTICS AND SPACE ADMINISTRATION

TECHNICAL MEMORANDUM X-333

LOW-SPEED INVESTIGATION OF THE EFFECTS OF WING FLAP DEFLECTION AND HORIZONTAL-TAIL CONFIGURATION ON THE LONGITUDINAL AERODYNAMIC CHARACTERISTICS OF AN AIRPLANE CONFIGURATION HAVING TAIL SURFACES OUTBOARD OF THE WING TIPS*

By William C. Hayes, Jr., and William C. Sleeman, Jr.

SUMMARY

A low-speed investigation has been made in the Langley 300-MPH 7- by 10-foot tunnel to determine the static longitudinal stability and control characteristics of a model having tail surfaces located outboard and rearward of the wing tips. The model had a 60° sweptback wing of aspect ratio 1.0, a 67-percent-semispan 15-percent wing-mean-aerodynamic-chord Fowler flap, and a full-span 10-percent wing-mean-aerodynamic-chord leading-edge flap. Effects of horizontal-tail size, planform, and dihedral were studied briefly. In addition, effects of partial-span leading-edge chord extensions and wing-tip span extensions were determined.

The basic model with flaps retracted had positive static longitudinal stability for trimmed conditions over the test angle-of-attack range which extended to 30°. A 30° deflection of the Fowler flap gave an increment in lift coefficient of about 0.20 but caused a significant loss of stability for lift coefficients above about 0.50. Addition of partial-span leading-edge chord extensions delayed the onset of the loss in stability from a lift coefficient of about 0.50 to about 0.70; however, at higher lift, the loss in stability was greater with the extensions on. Slightly higher values of trimmed lift-drag ratio were obtained for the model with the Fowler flap deflected 30° and the leading-edge flaps deflected 15° than were obtained for the basic model with these flaps undeflected for a range of lift coefficients above about 0.40.

---

*Title, Unclassified.

[redacted]

INTRODUCTION

An airplane configuration which is capable of achieving relatively high lift-drag ratios for supersonic-cruise conditions has been studied in several investigations which covered both subsonic and supersonic speed ranges (refs. 1 to 4). This type of airplane arrangement has the horizontal and vertical tail surfaces mounted on slender bodies and located outboard and rearward of the wing tips. A study of the basic concepts and some supporting experimental results for this type of configuration are presented in reference 1, and experimental results for some general research outboard-tail models at both supersonic and subsonic speeds are presented in references 2 to 4.

L 9 6 2

Results on the outboard-tail models at supersonic speeds (refs. 2 and 4) indicated that relatively high lift-drag ratios could be obtained for trimmed conditions over a fairly large range of low-lift static margins. Results for one model (ref. 4) indicated that the trimmed lift-drag ratios were essentially invariant with Mach number at a value of about 6.1 for a static margin of approximately 13 percent mean aerodynamic chord for Mach numbers between 2.30 and 4.06. Pitching-moment data at both subsonic and supersonic speeds showed, however, that static longitudinal instability occurred at moderate lift coefficients for the models reported in references 2 to 4. The effects of wing sweep and horizontal-tail size on low-speed longitudinal stability characteristics of an outboard-tail model were determined in the investigation of reference 3 and showed that the pitching-moment variation with lift could be improved somewhat by changes in tail size and reduction of the wing sweep; however, these improvements were not as large as would be desirable. The present investigation was therefore undertaken to continue the study of modifications for improvement of longitudinal stability and also to determine the characteristics with lift flaps deflected for simulation of low-speed flight conditions.

The present investigation of longitudinal aerodynamic characteristics was made in the Langley 300-MPH 7- by 10-foot tunnel over an angle-of-attack range to 30°. The model used in this investigation had a 60° sweptback wing of aspect ratio 1.0 equipped with 67-percent-semispan 15-percent wing-mean-aerodynamic-chord Fowler flap and a full-span 10-percent wing-mean-aerodynamic-chord leading-edge flap. The effects of horizontal-tail size were briefly studied with the basic tail and a smaller tail of the same planform. Effects of tail planform were investigated with a rectangular tail and two tapered tails, one having an unswept half-chord and the other an unswept trailing edge. In addition, the effects of wing leading-edge chord extensions and wing-tip span extensions were determined.

SYMBOLS

The system of axes used in this investigation is shown in figure 1 with an indication of the positive direction of forces, moments, and angular displacements. The moment-reference center was located 53.69 inches from the nose and corresponded to the 50-percent mean-aerodynamic-chord point of the wing alone. All coefficients presented herein are based on the area, span, and mean aerodynamic chord of the composite planform of the wing and the basic horizontal tail.

C_L lift coefficient, $\frac{\text{Lift}}{qS}$

C_D drag coefficient, $\frac{\text{Drag}}{qS}$

ΔC_D drag correction for fuselage base pressure

C_m pitching-moment coefficient, $\frac{\text{Pitching moment}}{qS\bar{c}}$

L/D lift-drag ratio

b_w span of wing alone, ft

$\bar{c}$ reference mean aerodynamic chord based on composite wing and basic horizontal tail, 2.08 ft

$\bar{c}_h$ mean aerodynamic chord of horizontal tail, ft

$\bar{c}_w$ mean aerodynamic chord of wing alone, ft

q free-stream dynamic pressure, lb/sq ft

S reference area of wing plus area of basic horizontal tail (not including area of trailing-edge extension), 6.84 sq ft

S_h area of horizontal tail, sq ft

S_w area of wing alone, sq ft

α angle of attack of fuselage center line, deg

ϵ downwash angle, deg

δ_f deflection of Fowler flap measured perpendicular to flap hinge line (positive when trailing edge is down), deg

δ_h deflection of horizontal tail with respect to fuselage center line (positive when trailing edge is down), deg

δ_n deflection of leading-edge flap with respect to wing chord in free-stream direction (positive when leading edge is up), deg

Γ_h dihedral angle of horizontal tail, deg

Λ sweepback angle, deg

Model-component designations:

F fuselage

W wing

O wing-tip bodies

V vertical tails

$H_1, H_2, \ldots H_5$ horizontal tails

L 962

MODEL AND APPARATUS

The model (figs. 2 to 5) used in this investigation consisted of a mahogany fuselage and wing-tip bodies with aluminum wing and tail surfaces. The wing-tip bodies were deflected 3° nose down with respect to the fuselage center line. The wing had 60° sweepback at the leading edge, an aspect ratio of 1.0, a taper ratio of 0.64, and a flat-plate airfoil section $0.02\bar{c}$ thick with a rounded leading edge and a beveled trailing edge. An extension was fitted to the wing trailing edge as shown in figure 2.

The planforms of the five horizontal-tail configurations used in the investigation are shown in figure 3. The basic horizontal tail H_1 had 60° sweepback at the leading edge and an area 25.70 percent of the wing area. The horizontal and vertical tail surfaces were made of 1/4-inch-thick aluminum plate with a rounded leading edge and a beveled trailing edge and with the exception of the area ratio for tail H_2 had the same ratio of tail area to wing area, $S_h/S_w = 0.257$. Horizontal

CONFIDENTIAL

tail H_2 had an area ratio $S_h/S_w = 0.183$. All horizontal tails could be deflected about a hinge axis perpendicular to the center line of the wing-tip body as shown in figure 2.

A few tests were made to investigate effects of 15° dihedral in the basic horizontal tail. For these tests the exposed root of the horizontal tail touched the surface of the wing-tip body in approximately the same place as for the basic horizontal tail with 0° dihedral. The vertical tails were identical in planform to the basic horizontal tail H_1.

Provisions were made to droop the leading-edge portion of the wing 15° with respect to the wing chord line in the free-stream direction about an axis located $0.10\bar{c}_w$ behind the leading edge as shown in figures 2 and 4. A Fowler flap having a span of $0.67b_w/2$ and a chord of $0.15\bar{c}_w$ was also incorporated in the model and could be deflected about its hinge line 15°, 20°, or 30° (figs. 2 and 4). When deflected, this flap was supported in most of the tests at the outboard end by brackets on the lower surface of the wing.

A few tests were made to determine effects of a wing leading-edge chord extension which was attached to the outboard one-third of the wing and had airfoil sections identical to the wing leading edge (fig. 5). Some wing-tip span extensions were also studied by attaching 1/8-inch-thick metal plates to the outer surface of the wing-tip bodies (fig. 5).

Surveys of the flow field behind the model were made with a tuft grid placed approximately 1 foot downstream of the most rearward part of the model in order to observe the angularity caused by the wing-tip vortex throughout the angle-of-attack range. Photographs (fig. 6) of the tuft grid were made at a tunnel dynamic pressure of approximately 5 pounds per square foot. For these photographs the horizontal and vertical tail surfaces were replaced by 1/8-inch-diameter rods which extended normal to the center line of the wing-tip bodies out to the tip location of the tail surfaces. Downwash and sidewash angles are indicated by the vertical and horizontal projections of the woolen tufts. The apparent angularity around the edges of the tuft grid is due to parallax. The trailing edges of the wing, flap, and trailing-edge extension are indicated in figure 6 by painted strips along these edges, about 1/4 inch wide. The center lines of both the fuselage and the wing-tip bodies are also indicated by painted strips.

CONFIDENTIAL

TESTS AND CORRECTIONS

The present investigation was made in the Langley 300-MPH 7- by 10-foot tunnel at a dynamic pressure of 57.5 pounds per square foot which corresponds to an airspeed of about 150 miles per hour. The test conditions produced a test Reynolds number of approximately 3.0×10^6 based on the mean aerodynamic chord of the combined wing and basic horizontal tail. The test angle-of-attack range was from -4° to approximately 30°.

Blockage corrections were computed by the method of reference 5 and were applied to the free-stream dynamic pressure. Jet-boundary corrections as computed by the method of reference 6 were added to the angles of attack and drag coefficients. In the determination of these corrections, the wing and horizontal tail were considered as a single lifting surface. Corrections for tunnel buoyancy effects were also applied to the data.

L 9 6 2

PRESENTATION OF RESULTS

Figures presenting the results of a low-speed investigation of an outboard-tail model are summarized as follows:

	Figure
Tuft-grid surveys behind model	6
Effect of Fowler flap bracket on wing lower surface	7
Effect of Fowler flap deflection	8
Effect of horizontal-tail deflection for -	
$\delta_f = 0^\circ$; $\delta_n = 0^\circ$	9(a)
$\delta_f = 30^\circ$; $\delta_n = 0^\circ$	9(b)
$\delta_f = 30^\circ$; $\delta_n = -15^\circ$	9(c)
Photographs of wing-surface tufts	10
Effect of wing chord extension on -	
Longitudinal aerodynamic characteristics	11(a)
Pitching-moment characteristics	11(b)
Effect of reduction in horizontal-tail area	12
Effect of horizontal-tail dihedral	13
Effect of horizontal-tail planform	14
Effect of wing-tip span extension	15
Drag corrections for fuselage base pressure	16
Effect of flap deflection on trimmed lift-drag ratios	17

DISCUSSION

One of the basic reasons for placing the horizontal tail surfaces of an airplane outboard of the wing tips is to take advantage of the upwash field generated by the wing-tip vortex which may allow the horizontal tail to carry an upload for trim while inclined negatively with respect to the free-stream direction during trimmed flight. This condition would be expected to yield a drag reduction due to trimming by virtue of the forward inclination of the resultant force vector on the horizontal tail. Since the magnitude of this drag reduction would depend on the strength of the upwash field sensed by the horizontal tail, it would be desirable to locate the tail in the region of strongest upwash associated with the cruise angle of attack in order to realize the highest trimmed lift-drag ratio attainable for the configuration. Test results at supersonic speeds (refs. 2 and 4) demonstrated the aforementioned possible gains in trimmed lift-drag ratio obtained by use of moderate negative values of horizontal-tail deflection; however, a large loss of stability at moderate lift coefficients was noted and is believed to have been caused by the emergence of the horizontal tail from the high upwash region as the angle of attack increased above that for cruise. This problem of longitudinal instability was also encountered in the low-speed tests of an outboard-tail configuration reported in reference 3. The nature of the problem of large stability changes occurring as a result of relative movement of the upwash field of the wing-tip vortex with respect to the horizontal tail suggested that a better understanding of the aerodynamic characteristics of the configuration could be gained from observations of a tuft grid behind the model.

Tuft-Grid Surveys

Photographs of the tuft grid presented in figure 6 show the expected angularity increase with increasing angle of attack; however, the inward movement of the tip vortex associated with increasing angle of attack which has been encountered on wings having fairly large sweepback was not so marked on the present model. Additional surveys with a single tuft attached to a slender probe showed that when the flaps were undeflected the wing-tip vortex originated at the point where the wing leading edge joined the wing-tip body, trailed along the juncture of the inner face of the wing-tip body and the upper surface of the wing, and was shed from a point on this juncture in the vicinity of the wing trailing-edge extension throughout the positive angle-of-attack range. Deflection of the wing flaps (fig. 6(b)) caused the whole vortex pattern to shift downward and at low angles of attack to be shed largely from the outboard edge of the flap. At higher angles of attack the flap vortex merged with the wing-tip vortex and again appeared to trail from

the inboard side of the wing-tip body. Differences in the vortex location with the flaps deflected and undeflected is indicated in the force data (fig. 8) which shows somewhat higher stability near zero lift when the flaps are deflected.

Formation of the wing-tip vortex about the inboard side of the wing-tip body would be expected to produce less upwash in the horizontal-tail region than would be produced if the vortex center was on the outer edge of the body. With this thought in mind, some wing span extensions were attached to the wing-tip bodies in order to determine the gains in lift coefficient that might occur from shifting the origin of the wing-tip vortex outboard. An outboard shift of the vortex would be expected to increase both the wing effective aspect ratio and the upwash over the horizontal tail. Effects of a 2-inch span extension on the flow field behind the model may be seen in figure 6(c) which shows the model with an extension on the right wing only. A comparison of the flow field behind the left wing and the right wing shows that the tip extension was effective in moving the wing-tip vortex outboard. For the highest angle of attack shown, however, the center of the vorticity at the grid appeared to be located at about the same spanwise position for both wing panels, although the angularity appeared to be more extensive outboard of the right wing tip.

L 9 6 2

Aerodynamic Characteristics of the Basic Configuration

Effect of wing flap deflection.- The outboard end of the Fowler flap was supported by a bracket (see figs. 2 and 5), and a few tests were made to determine if the bracket had an adverse effect on the model aerodynamic characteristics. Test results with the bracket on and with it replaced by a small metal fitting showed very little overall effect of the bracket (fig. 7), and the small effect shown at high angles of attack with the bracket on was favorable; the bracket was therefore attached to the model for all subsequent tests.

Effects of incremental deflection of the Fowler flaps on longitudinal aerodynamic characteristics of the model are presented in figure 8. Deflections of the flap were accompanied by constant increments of lift coefficient ($\partial C_L/\partial \delta_f = 0.0067$ per deg) through the angle-of-attack range to about 20°. Although the minimum drag increased with increased Fowler flap deflection, the drag coefficient at a given lift coefficient above approximately 0.50 was less for a flap deflection of 30° than for smaller deflections. Therefore, a flap deflection of 30° was used for all tests with the flaps deflected. Deflection of the flap increased the stability at low lift and caused somewhat smaller variations in stability with lift through the lift-coefficient range to about 0.60 (fig. 8). For lift coefficients above about 0.90, however, deflection

of the Fowler flaps caused a marked loss of stability. The longitudinal instability shown in figure 8 at high lift with flaps deflected is believed to be the result of stalling of the horizontal tail inasmuch as pitching moments obtained with high negative horizontal-tail deflections (fig. 9(a)) showed an increase in stability at the highest lift coefficients.

Effect of horizontal tail.- The effect of horizontal-tail deflection on the longitudinal aerodynamic characteristics of the model with undeflected leading-edge and trailing-edge flaps ($\delta_f = 0^\circ$; $\delta_n = 0^\circ$) is shown in figure 9(a). Negative (leading edge down) deflection of the horizontal tails was accompanied by nearly constant decrements of lift coefficient through the test angle-of-attack range to about 20°. Above an angle of attack of 20°, horizontal-tail stall is evidenced in the lift data and by the marked reduction in stability at the smaller angles of horizontal-tail deflection. The pitching-moment characteristics also indicated (fig. 9(a)) that the basic horizontal tail was an effective longitudinal control for angles of attack up to 25° and that the model was statically stable for trimmed conditions to an angle of attack of at least 30° for an assumed center-of-gravity location which gave a static margin near zero lift of approximately 12 percent mean aerodynamic chord.

Deflection of the leading-edge and trailing-edge flaps produced an increment of lift coefficient at a given angle of attack of approximately 0.20 through the test angle-of-attack range and a decrement of pitching-moment coefficient which was about equal to that produced by 6° or 8° (depending on the angle of attack) of negative deflection of the horizontal tail (figs. 9(a) and 9(c)). Although deflection of the flaps delayed significant nonlinearities in the pitching-moment curves to an angle of attack of about 10°, an unfavorable effect of flap deflection on longitudinal stability was indicated above this angle of attack. For the center of moments selected, the model was about neutrally stable for trimmed conditions over an angle-of-attack range from about 12° to 26°. The pitching moments at higher angles of attack showed an increase in stability with the highest negative setting tested.

The tuft-grid surveys (see fig. 6) did not provide an explanation for the loss in stability above 10° angle of attack when the flaps were deflected inasmuch as the tail appears well immersed in the upwash field at $\alpha = 16.3^\circ$ (fig. 6(b)). Examination of pitching moments obtained with the horizontal tail removed, however, shows a large unstable break for angles of attack above about 12° (fig. 9(c)) which corresponds closely to the angle of attack of the complete model at which loss in stability occurs. Inasmuch as the tail contribution $\left[(C_m)_{\text{tail on}} - (C_m)_{\text{tail off}}\right]$ was fairly linear with respect to changes

in angle of attack throughout most of the angle-of-attack range, the loss of stability near 12° can be attributed to the characteristics of the wing-body combination when the flaps were deflected.

Tuft Study of Flow Over Wing Surface

Flow over the model was studied by means of wool tufts attached by clear cellophane tape to the upper surface of the left half of the model. Photographs of the tufts were made through a window in the ceiling of the tunnel and some of these photographs are presented in figure 10 to show effects of flap deflection on flow over the wing surface. Evidence of spanwise flow appeared at fairly low angles of attack (below 6°) and began near the leading edge with flaps retracted. Deflection of the leading-edge and trailing-edge flaps caused the spanwise flow to occur at a more rearward chordwise location. Deflection of flaps caused the spanwise flow to become stronger, more turbulent, and somewhat more extensive. With the flaps deflected, separated flow occurred at the juncture of the wing leading edge and the wing-tip body even at fairly low angles of attack, and the separation appeared to spread inward and rearward as the angle of attack increased. Loss of lift on an outboard segment of the wing leading edge would not of itself be expected to cause large changes in pitching moments because of the relatively short moment arm involved (see fig. 2); however, the separated flow coming from this source may cause a loss of lift over the rearward portions of the wing which would cause a destabilizing pitching-moment increment. In addition, visual observations of the surface tufts and, to a lesser extent, the photographs of figure 10 showed that a large downward flow existed around the inboard edge of the trailing-edge extension with the flaps deflected. A down load on the extension could cause a loss of stability if this down load increased with angle of attack. It is possible, therefore, that this down load and the effects resulting from separation in the region of the leading edge of the wing tip were the main contributors to the loss of stability encountered on this model with the flaps deflected.

L 9 6 2

Modifications to the Basic Configuration

Effect of leading-edge chord extensions.- Inasmuch as the longitudinal-stability problems of this model with flaps deflected appeared to be in the wing-body characteristics, a few tests were made with leading-edge chord extensions in place (see fig. 5) in attempts to improve the flow over the wing. Test results obtained with a 1/3-semispan chord extension are presented in figure 11(a) and effects of the chord extensions on pitching moments are shown in figure 11(b). The results presented in figure 11 are consistent with past experience on application of chord extensions to wings of somewhat higher aspect

ratio. Use of the leading-edge chord extensions delayed the lift coefficient at which the stability became about neutral from approximately 0.50 (basic model) to 0.70 (model with extensions) for the maximum horizontal-tail deflection of the test. (See fig. 11(b).) This stability improvement is shown in the tail-off results for which the extensions made the pitching-moment curve more linear at low lift and delayed the break somewhat. The results presented in figure 11 also show that even though the extensions delayed the break in the pitching-moment curve, when the break did occur, it was somewhat more severe than that for the model with no leading-edge extensions. The use of the leading-edge chord extensions would, however, be beneficial from the standpoint of static longitudinal stability for the present configuration with deflected flaps for angles of attack below 18°.

Effects of changing the horizontal-tail geometry.- The test results presented in reference 3 indicated that some reduction in the variation of stability with lift could be obtained by reducing the tail size. One of the smaller tails used in the tests of reference 3 was tested on the present model (see tail H_2, fig. 3) with flaps deflected, and the results are presented in figure 12. These data show the expected reduction in stability when the tail area was reduced; however, the overall change of stability with lift coefficient was approximately the same for both tails. The absence of stability benefits from the small tail on the present model is understandable in view of the fact that adverse stability effects on the present model with flaps deflected originated in the tail-off characteristics whereas those for the model of reference 3 originated primarily in the tail contribution.

The geometric modifications incorporated in the present model appeared to have been effective in alleviating longitudinal-stability problems arising from losses in tail contribution to stability shown in reference 3. Several different modifications were made, and it is not possible on the basis of present data to assess the contribution of each to the improvements in the present model. One of the considerations involved in the present configuration was to locate the horizontal tail above the chord plane of the wing by inclining the wing-tip bodies up at the rear which would tend to keep the tail in a high upwash field to higher angles of attack than if the tail were on the wing chord plane. Another possible means for elevating the horizontal tail is to put dihedral in the tail. Some results for the present model with flaps retracted which show effects of 15° tail dihedral are presented in figure 13. These results show almost no effect of dihedral on stability at low lift, and somewhat less stability was obtained at higher lift with dihedral than without dihedral. The results of figure 13 and an examination of the flow fields shown in figure 6 suggest that the use of tail dihedral is not an effective means for placing the tail in high upwash when the vortex center is above the tail because the sidewash

component of the wing-tip vortex flow when directed outward would reduce the angle of attack of a tail having positive dihedral. Inclining the wing-tip body as in the present model or "bending" the rear of the wing-tip body upward as in the model of reference 4 may offer a more effective means of raising the tail to remain in high effective upwash than using positive dihedral in the tail.

A few tests were made to determine how sensitive the overall longitudinal stability characteristics of the model were to variations in the horizontal-tail planform, and these results are presented in figure 14. The horizontal tails had the same planform area and were pivoted about the quarter-chord of the tail mean aerodynamic chord as shown in figure 3. The differences in pitching-moment characteristics shown in figure 14 with -3° horizontal-tail deflection may be attributed to effects of planform on the stall characteristics of the tails. The angle of attack at which the pitching-moment curve reversed slope was, for example, increased as the leading-edge sweep angle of the tail increased. Results obtained with a tail deflection of -15° showed little effect of tail planform up to an angle of attack of about 25°, and the basic 60° swept-back tail appeared to provide the best tail planform of the several planforms tested.

L 9 6 2

Effect of wing-tip span extensions.- The purpose of the wing-tip span extensions was briefly indicated in the discussion of tuft-grid surveys. Force data obtained with two tip extensions are presented in figure 15. Addition of the 2-inch span extension increased the lift-curve slope of the model as expected, and, with the horizontal tail removed, the lift increment contributed by this extension at 15° angle of attack was about the same as the lift increment arising from 20° Fowler flap deflection. (See fig. 8.) The increase in lift-curve slope for the wing-body configuration was accompanied by an increase in longitudinal stability when the wing-tip extensions were added inasmuch as essentially all of the added area was behind the moment reference. The results shown in figure 15 for the model with the tail removed would be expected from the fact that lifting area was added to the wing which was not accounted for in the reference area used in reducing the data. When the lift coefficients for the model with the extensions are based on the reference area plus the extension area, the lift-curve slope at low angles of attack would be about the same as without the extensions. The lift-curve slope for angles of attack above about 8° would be somewhat higher, however, for the model with the tip extensions than for the basic model.

Test results for the complete model (fig. 15) show that the lift benefits, obtained by adding the wing-tip extensions to the wing-body configuration, were reduced and the longitudinal stability characteristics were adversely affected when the extensions were added to the model with the tail on. These adverse effects were caused by a loss

in tail contribution which occurred probably as a result of a decrease in effective upwash gradient $\partial\epsilon/\partial\alpha$ and a reduction in tail effectiveness $\partial C_m/\partial\delta_h$. Apparently a region of high downwash existed behind the tip extensions and was so strong that its effect overcame effects of the increased upwash outboard of the extensions.

Effect of Flap Deflection on Trimmed Lift-Drag Ratios

Subsequent to completion of the tests made in this investigation, static pressures were surveyed over the base of the present model; however, these pressure measurements were not available when the data of the present study were computed. The results of this base pressure survey with flaps deflected and undeflected have been evaluated in terms of a base drag increment which can be used to correct the drag to conditions of free-stream static pressure acting over the base of the model. Base pressures were measured for only one tail deflection inasmuch as the tail was well removed from the model base and, therefore, would not be expected to have a large influence on the base pressures. These base drag corrections are presented in figure 16 and were applied to the drag data when the lift-drag ratios presented in figure 17 were evaluated.

Deflection of the wing trailing-edge flaps to obtain an increase in lift at a given angle of attack was accompanied by a negative pitching-moment increment (fig. 8). This pitching-moment contribution of the flaps was not large by comparison with more conventional airplane arrangements because the rearward location of the moment-reference center placed the assumed center of gravity only a short distance ahead of the incremental flap load. The negative pitching-moment increment that does exist, however, may require an incremental down load on the tail to trim at a given lift, the magnitude and direction of this load depending upon the shape of the pitching-moment curve. This incremental down load would, of course, have an adverse effect on lift-drag ratios, and therefore it is necessary to consider trimmed conditions when the effect of flap deflection is assessed in terms of airplane lift-drag ratios.

The very low stability above 12° angle of attack of the model with flaps deflected (fig. 9(c)) gave a wide range of possible trimmed lift coefficients between the two highest horizontal-tail deflections. Some additional tests were made in order to define more accurately the trimmed drag polars by selecting additional horizontal-tail deflections to fill in the existing gaps in needed information. Basic data from these additional tests are not presented herein; however, trimmed drag polars are presented in figure 17 in which these data have been used.

CONFIDENTIAL

Lift-drag ratios presented in figure 17 show that higher values of L/D for trimmed conditions were obtained with the Fowler flaps deflected 30° and the leading-edge flaps deflected 15° than were obtained with the flaps retracted for lift coefficients above about 0.40.

SUMMARY OF RESULTS

The results of a low-speed wind-tunnel investigation of the effects of wing flap deflection and horizontal-tail configuration on the longitudinal aerodynamic characteristics of an airplane configuration having tail surfaces outboard of the wing tips may be summarized as follows:

L 9 6 2

1. The basic model with flaps retracted which had a 60° sweptback wing of aspect ratio 1.0 had positive static longitudinal stability for trimmed conditions over the test angle-of-attack range up to 30° for an assumed center-of-gravity location which gave a static margin near zero lift of approximately 12 percent mean aerodynamic chord.

2. Deflection of the wing trailing-edge flaps caused some increase in stability at low lift but had an adverse effect on the stability of the model at moderate and high lift coefficients. This adverse effect of flap deflection on stability may be attributed to flow changes at the wing which caused the wing-body characteristics to become more unstable rather than being attributed to losses in the stability contribution of the tail.

3. A 10-percent wing-mean-aerodynamic-chord extension to the wing leading edge was attached to the outboard one-third of the wing, and this extension delayed the lift coefficient at which the stability became about neutral from approximately 0.50 (basic model) to 0.70 for the maximum flap deflection. Although the extension delayed the break in the pitching-moment curve, when the break did occur, it was somewhat more severe than that for the basic model.

4. A study of effects of horizontal-tail planform and dihedral indicated that the basic 60° sweptback tail with 0° dihedral was superior to several different tails of equal area but having very low sweepback angles and tapered or rectangular planforms.

5. Slightly higher values of trimmed lift-drag ratio were obtained for the model with the Fowler flaps deflected 30° and the leading-edge

CONFIDENTIAL

flaps deflected 15° than were obtained for the basic model with these flaps undeflected for a range of lift coefficients above about 0.40.

Langley Research Center,
National Aeronautics and Space Administration,
Langley Field, Va., June 23, 1960.

REFERENCES

1. Sleeman, William C., Jr.: Preliminary Study of Airplane Configurations Having Tail Surfaces Outboard of the Wing Tips. NACA RM L58B06, 1958.

2. Church, James D., Hayes, William C., Jr., and Sleeman, William C., Jr.: Investigation of Aerodynamic Characteristics of an Airplane Configuration Having Tail Surfaces Outboard of the Wing Tips at Mach Numbers of 2.30, 2.97, and 3.51. NACA RM L58C25, 1958.

3. Hayes, William C., Jr., and Sleeman, William C., Jr.: Low-Speed Investigation of the Effects of Horizontal-Tail Area and Wing Sweep on the Static Longitudinal Stability and Control Characteristics of an Airplane Configuration Having Tail Surfaces Outboard of the Wing Tips. NASA MEMO 6-11-59L, 1959.

4. Sleeman, William C., Jr., Church, James D., and Fournier, Roger H.: Aerodynamic Characteristics of a 60° Sweptback-Wing Airplane Configuration Having Tail Surfaces Located Outboard of the Wingtips at Mach Numbers of 2.30, 2.97, 3.51, and 4.06. NASA TM X-219, 1960.

5. Herriot, John G.: Blockage Corrections for Three-Dimensional-Flow Closed-Throat Wind Tunnels, With Consideration of the Effect of Compressibility. NACA Rep. 995, 1950. (Supersedes NACA RM A7B28.)

6. Gillis, Clarence L., Polhamus, Edward C., and Gray, Joseph L., Jr.: Charts for Determining Jet-Boundary Corrections for Complete Models in 7- by 10-Foot Closed Rectangular Wind Tunnels. NACA WR L-123, 1945. (Formerly NACA ARR L5G31.)

CONFIDENTIAL

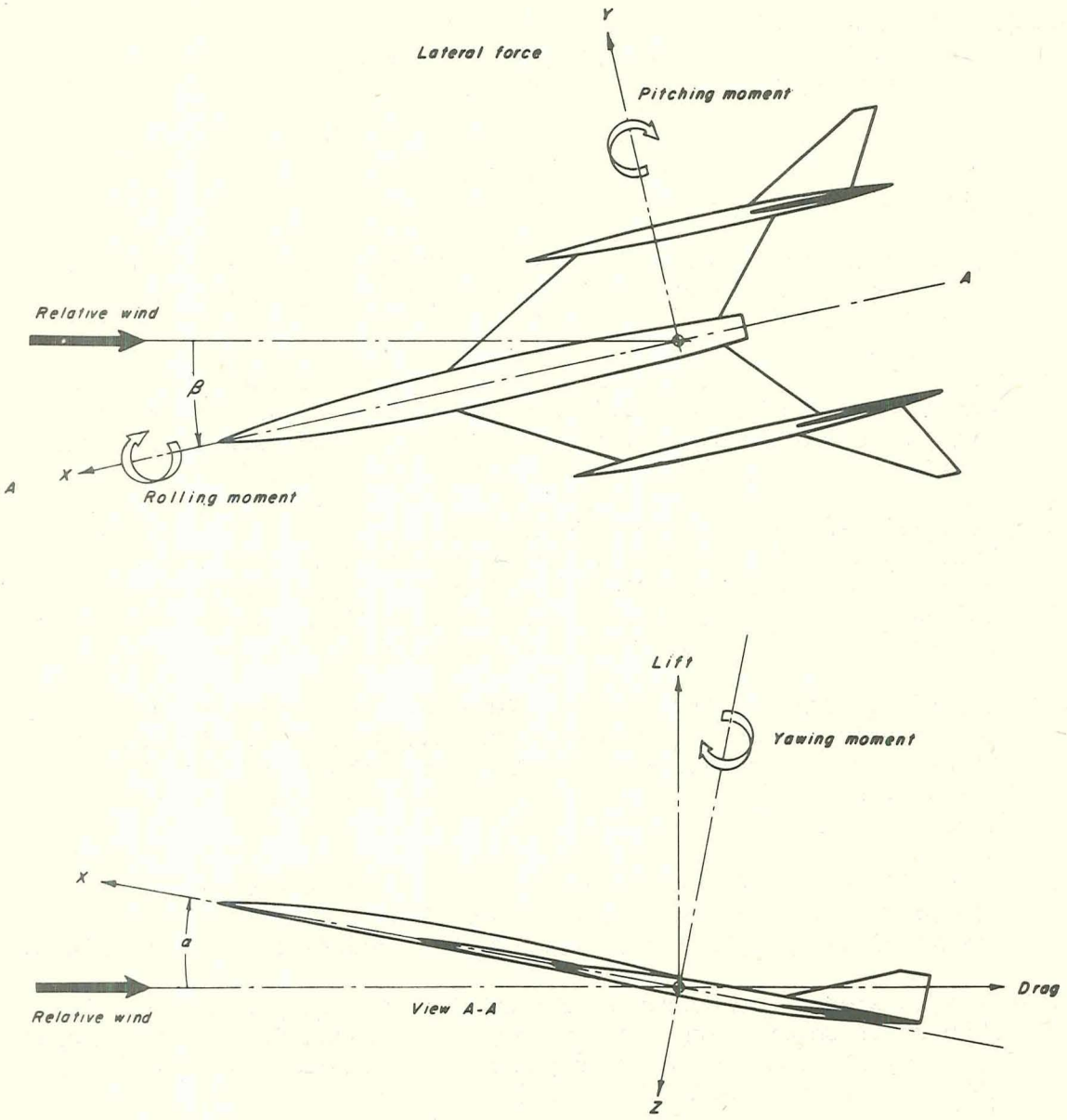

Figure 1.- System of axes used in presentation of data. Arrows indicate positive directions of forces, moments, and angles.

CONFIDENTIAL

I-962

3K

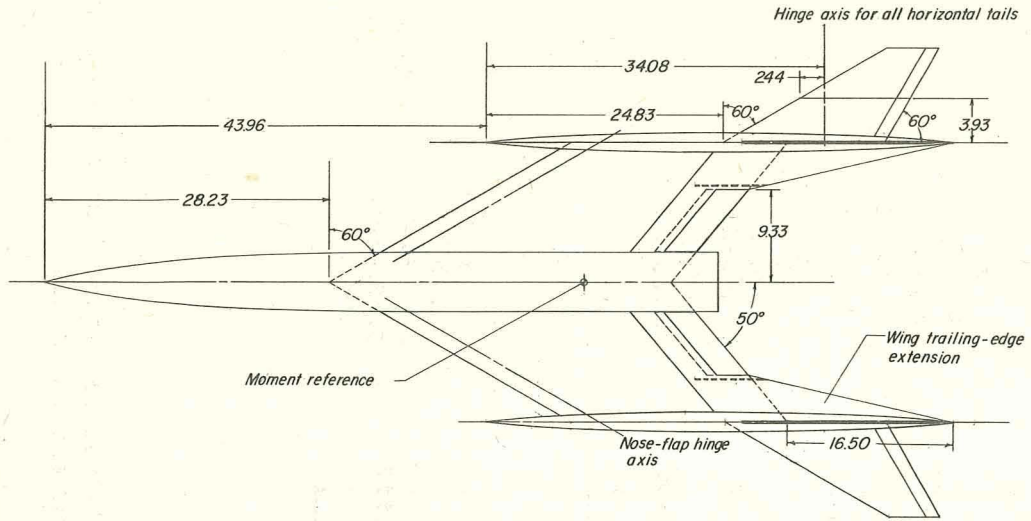

Wing geometry	
Area	784.00 sq in.
Root chord	34.25 in.
Tip chord	21.75 in.
Span	28.00 in.

Tail geometry	
Area (one tail)	100.66 sq in.
Root chord	16.08 in.
Tip chord	5.11 in.
Panel span	9.50 in.

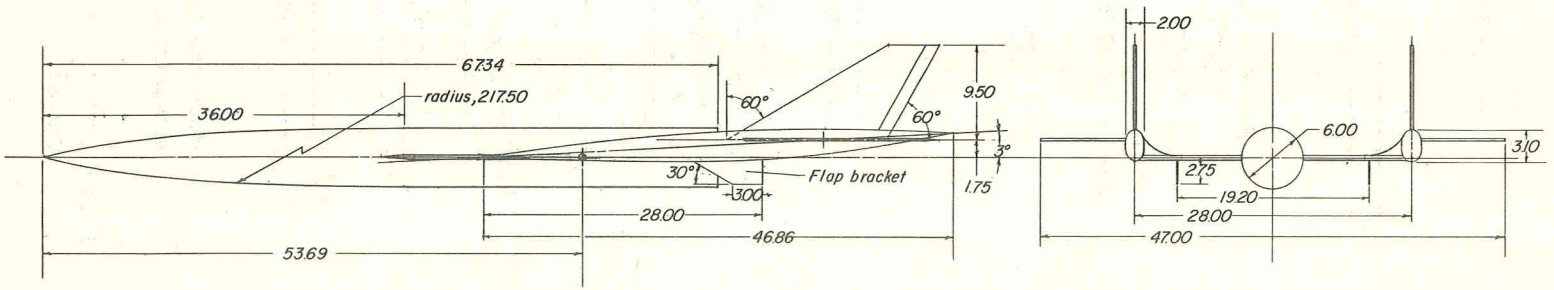

Figure 2.- Three-view drawing of the basic model. All dimensions are in inches.

CONFIDENTIAL

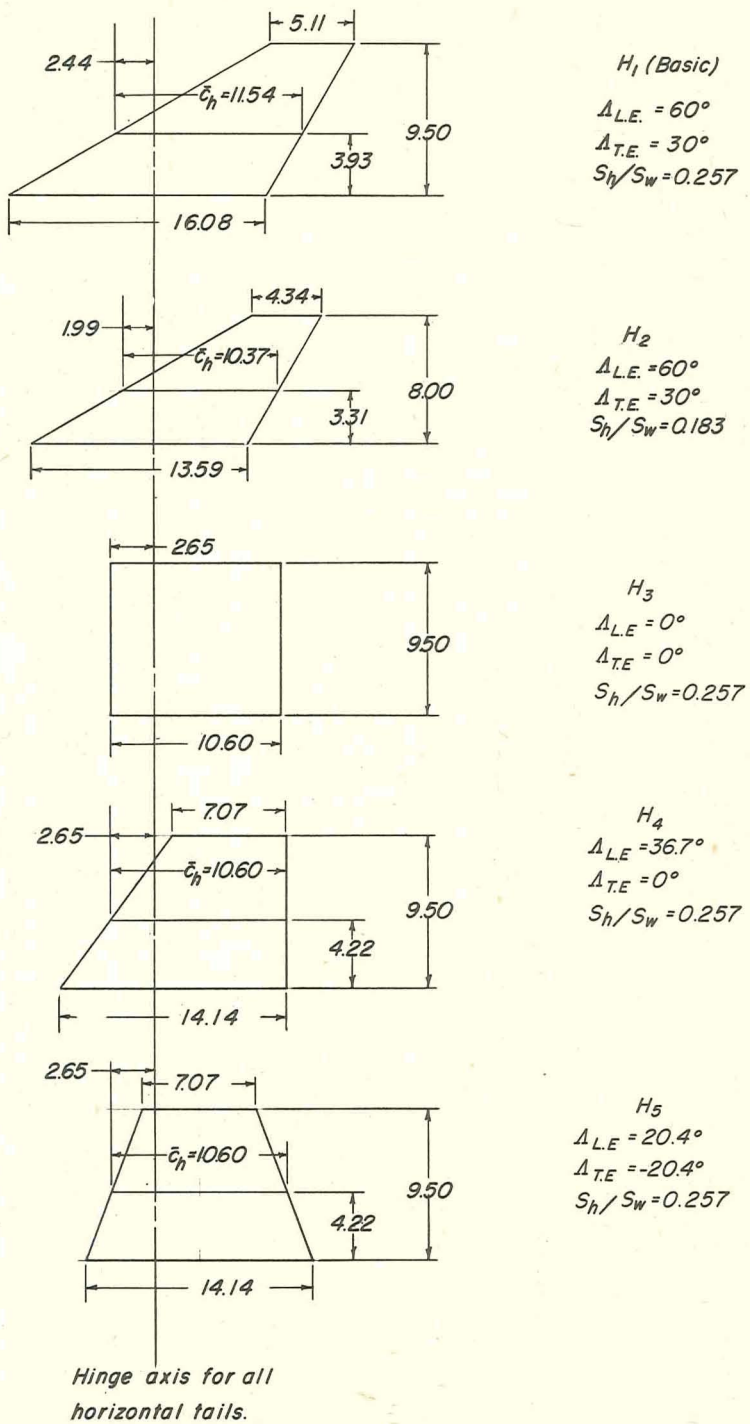

Figure 3.- Planforms of the horizontal-tail configurations tested on the model. All dimensions are in inches.

CONFIDENTIAL

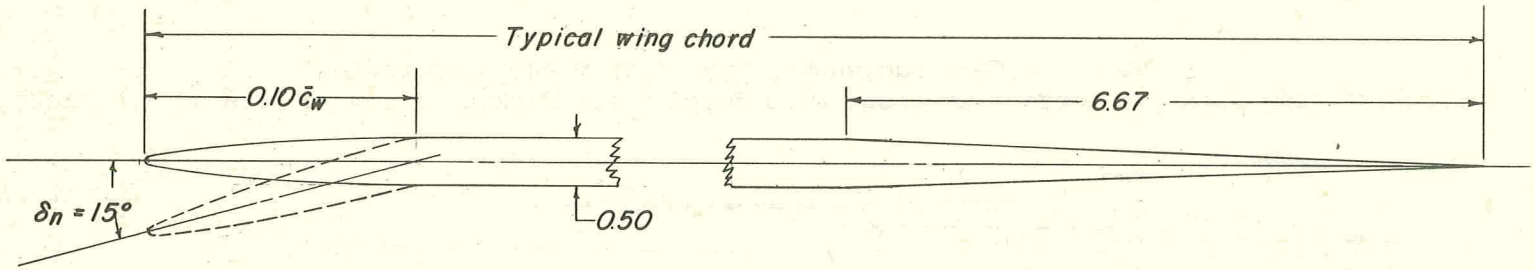

Typical wing section

(Parallel to free air stream)

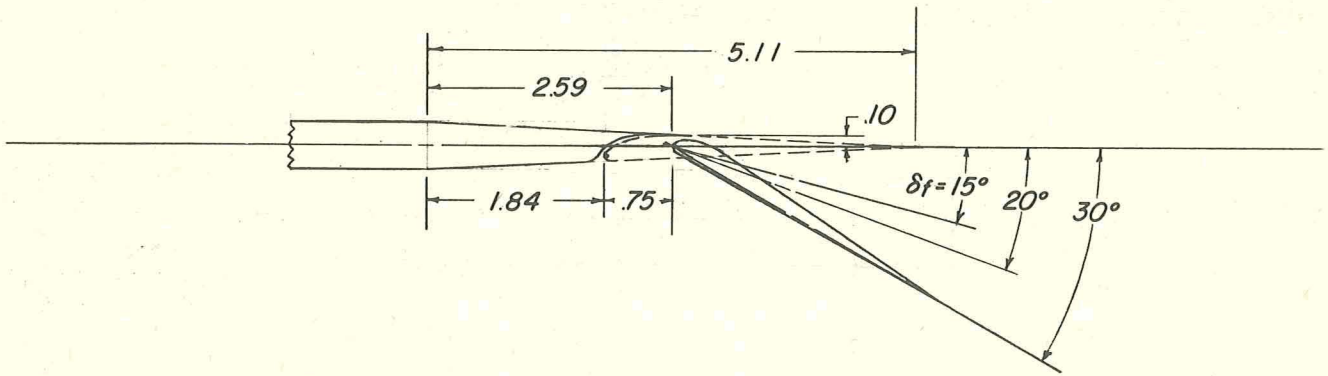

Typical flap section

(Perpendicular to flap leading edge)

Figure 4.- Typical wing sections showing some details of the leading-edge and Fowler flaps tested. All dimensions are in inches.

CONFIDENTIAL

CONFIDENTIAL

CONFIDENTIAL

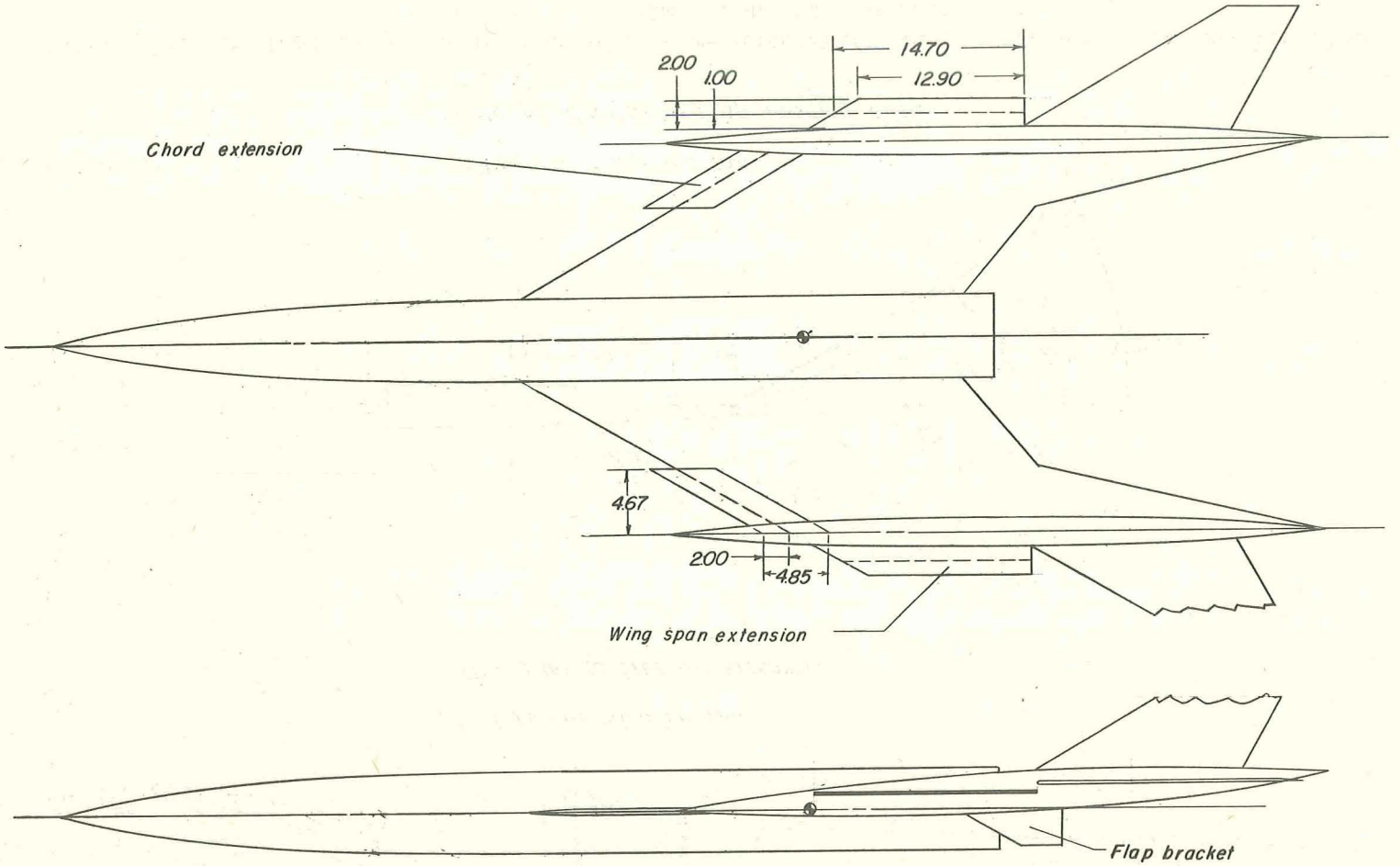

Figure 5.- Drawing of model showing the leading-edge chord extensions and wing span extensions tested on the model. All dimensions are in inches.

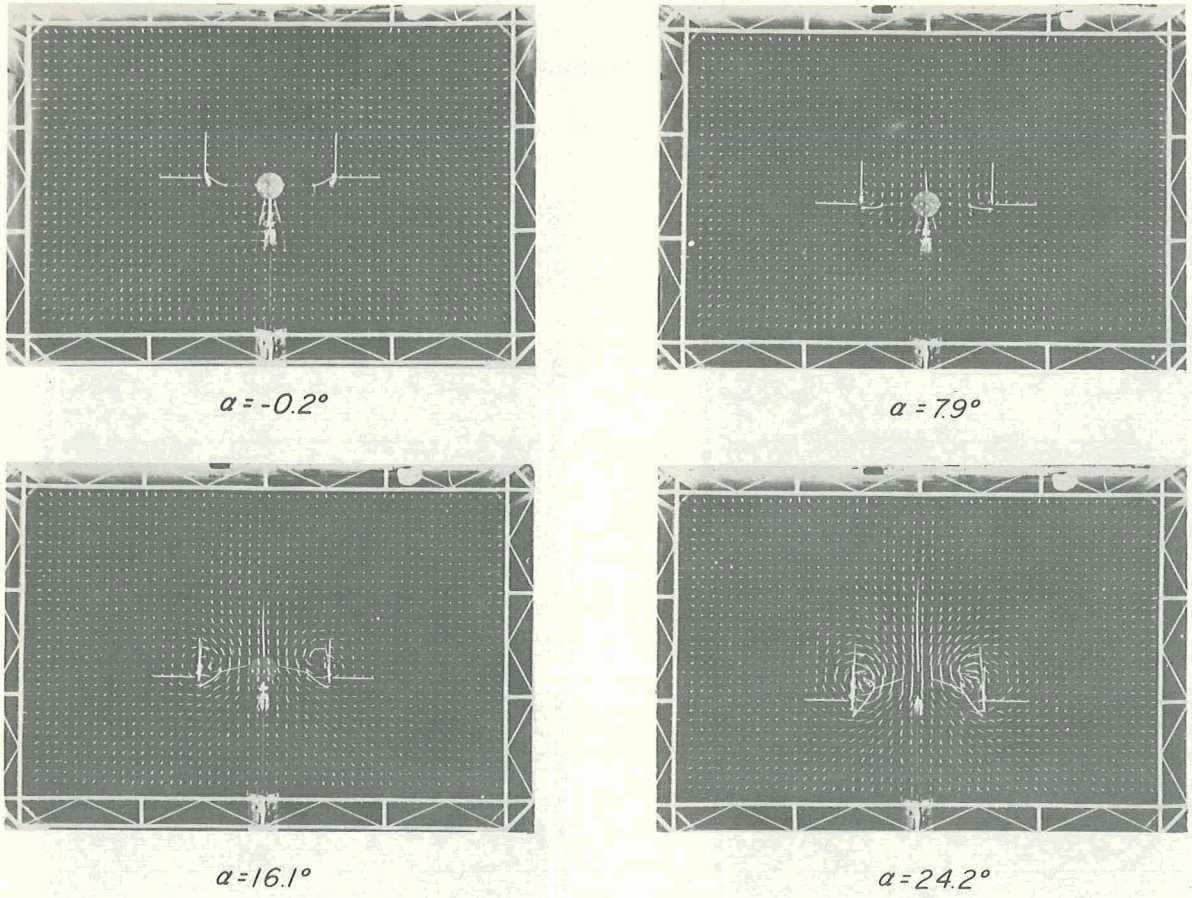

(a) Flaps undeflected. $\delta_f = 0^\circ$; $\delta_n = 0^\circ$.

L-60-2495

Figure 6.- Photographs of tuft grid behind the model. Tail surfaces are replaced by white, unswept rods to indicate region occupied by tails.

CONFIDENTIAL

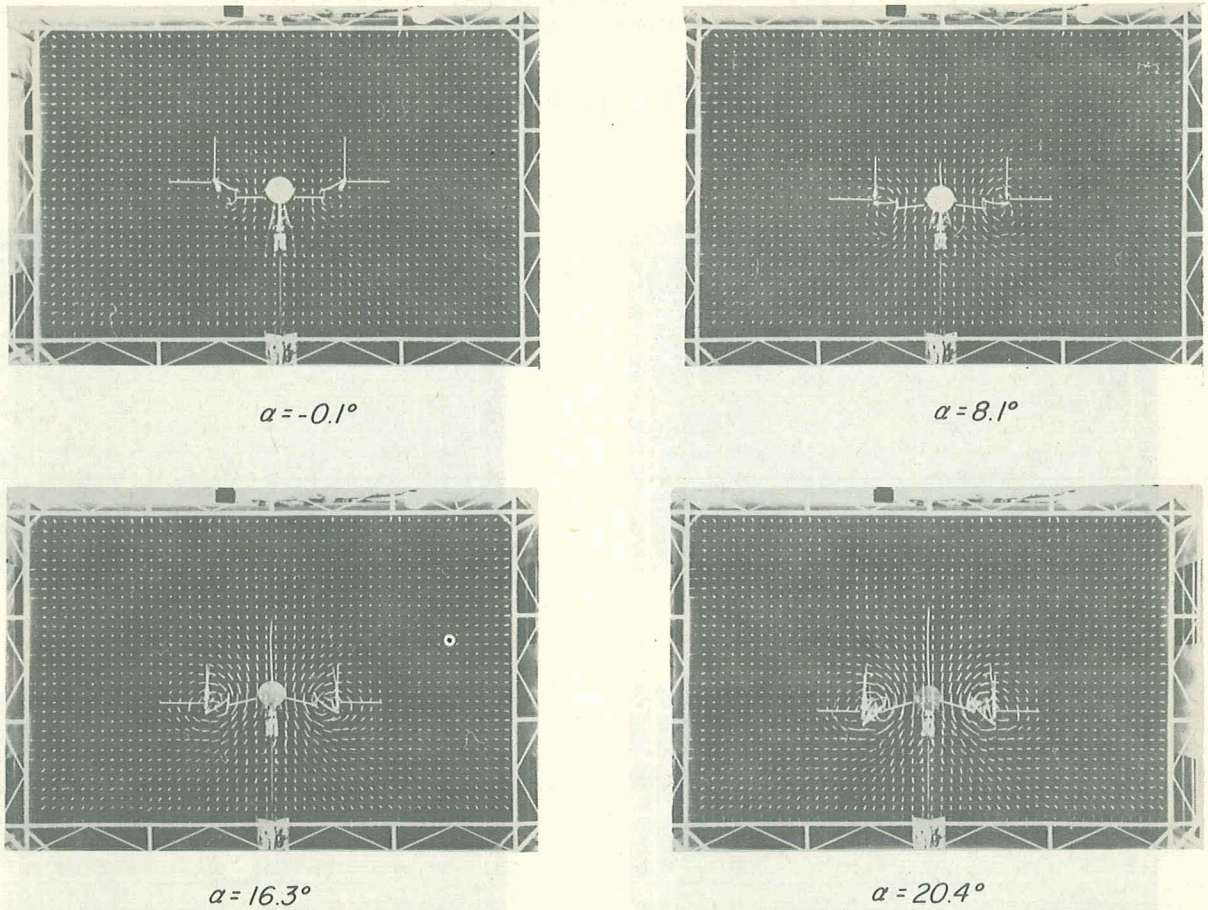

(b) Flaps deflected. $\delta_f = 30^\circ$; $\delta_n = -15^\circ$. L-60-2496

Figure 6.- Continued.

CONFIDENTIAL

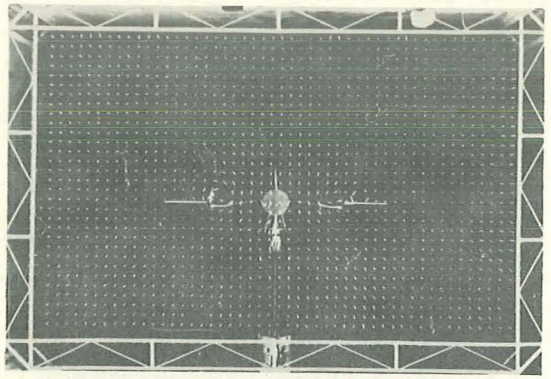

$\alpha = 7.9°$

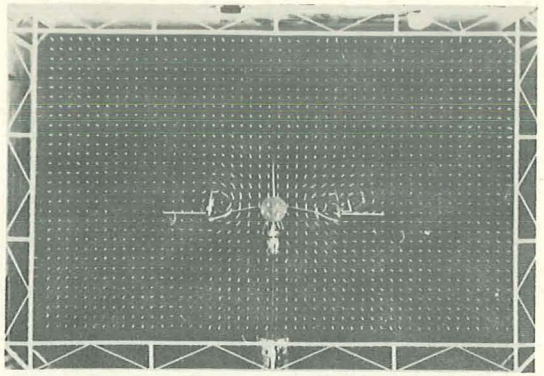

$\alpha = 12.0°$

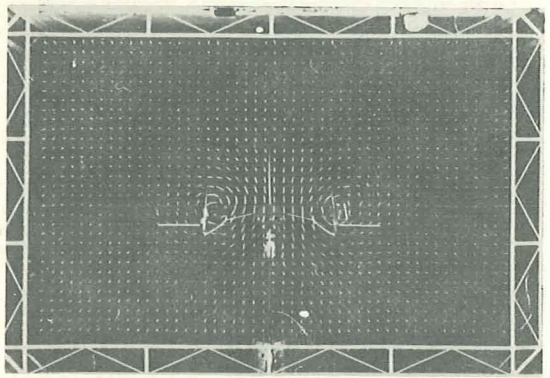

$\alpha = 16.1°$

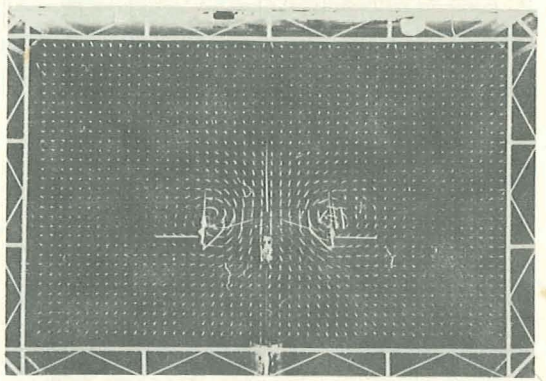

$\alpha = 20.1°$

(c) Flaps undeflected. 2-inch extension on right wing tip only. L-60-2497

Figure 6.- Concluded.

CONFIDENTIAL

CONFIDENTIAL

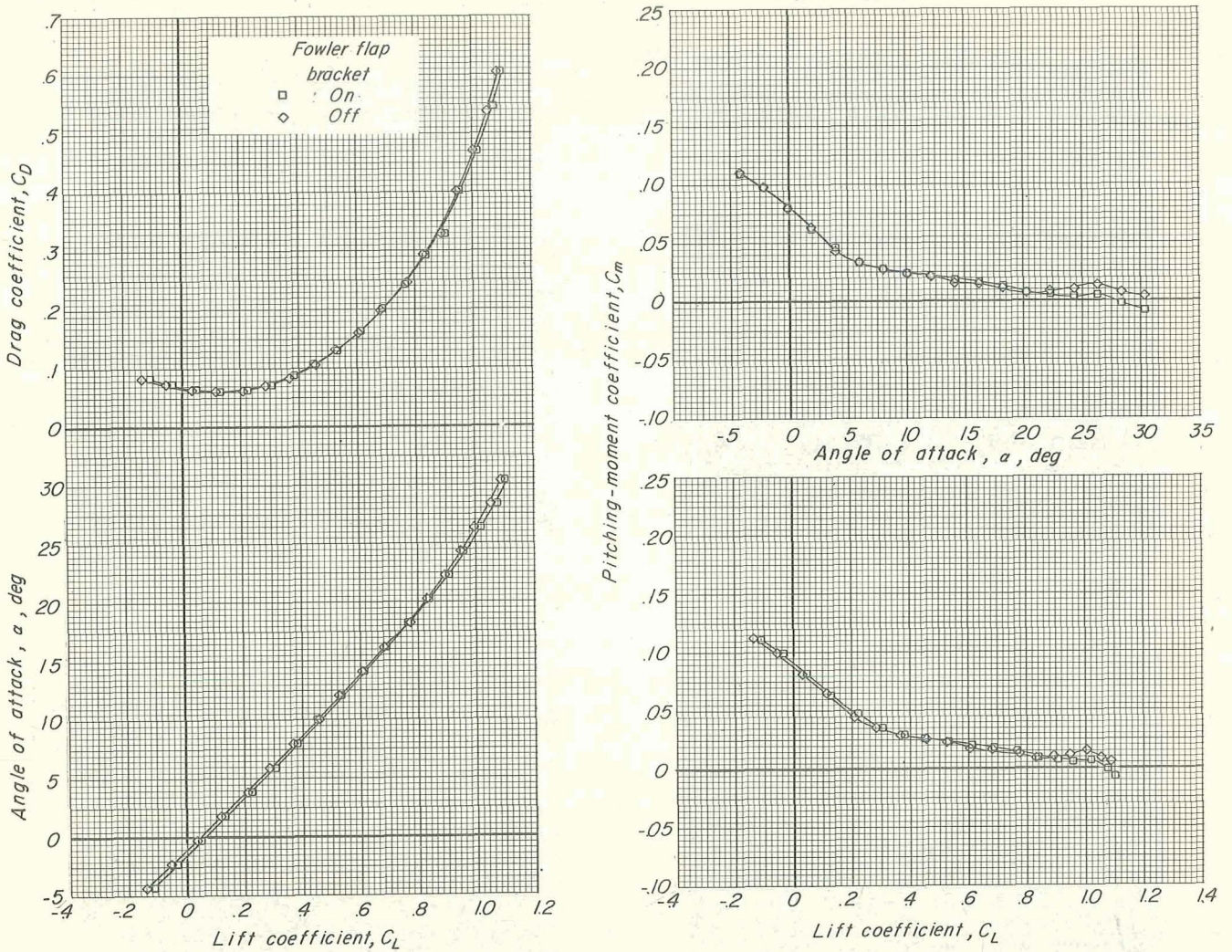

Figure 7.- Effect of Fowler flap bracket on the longitudinal aerodynamic characteristics of the basic model. $FWOVH_1$; $\delta_f = 30^\circ$; $\delta_h = -15^\circ$; $\delta_n = 0^\circ$.

CONFIDENTIAL

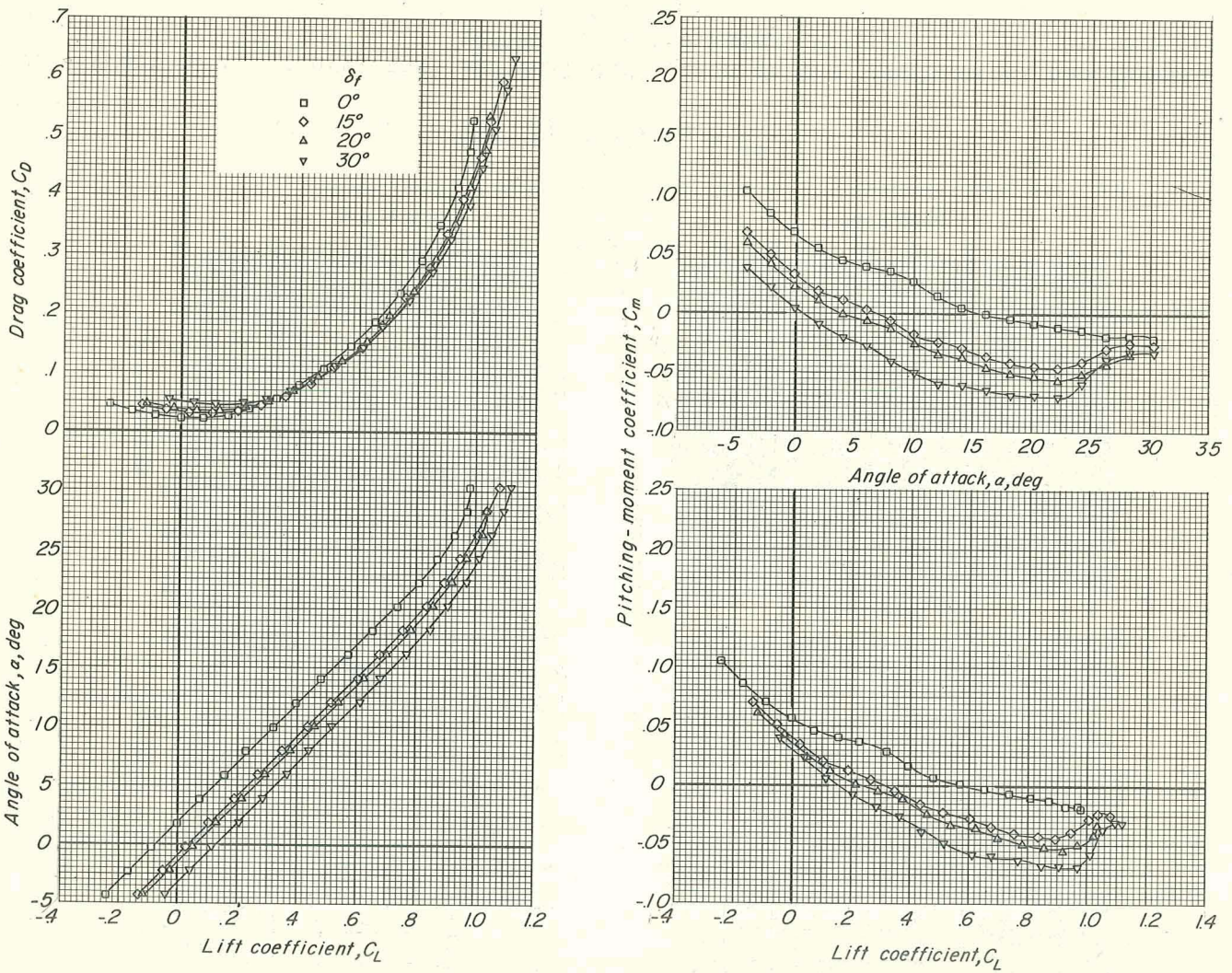

Figure 8.- Effect of Fowler flap deflection on the longitudinal aerodynamic characteristics of the model. $FWOVH_1$; $\delta_h = -6^\circ$; $\delta_n = 0^\circ$.

CONFIDENTIAL

CONFIDENTIAL

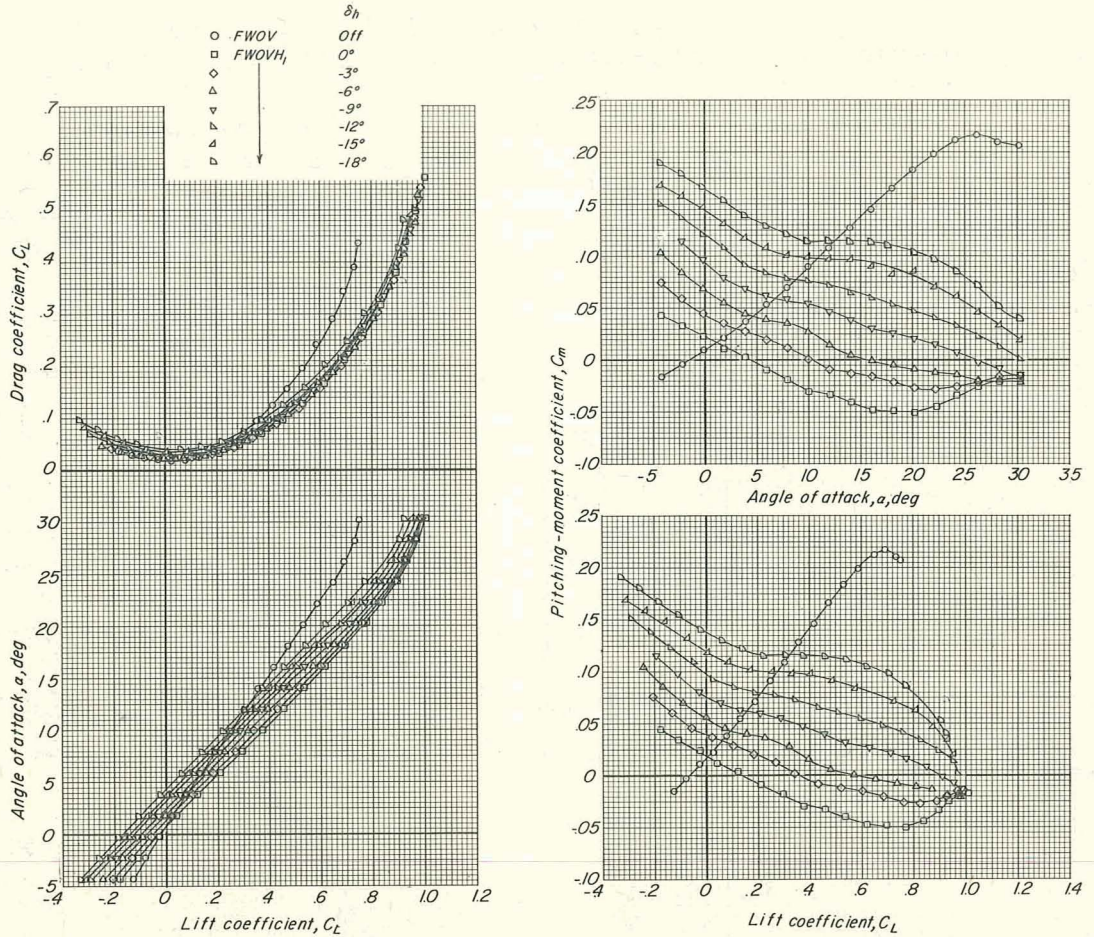

(a) $\delta_f = 0^\circ$; $\delta_n = 0^\circ$.

Figure 9.- Effect of horizontal tail and tail deflection on the longitudinal aerodynamic characteristics of the model.

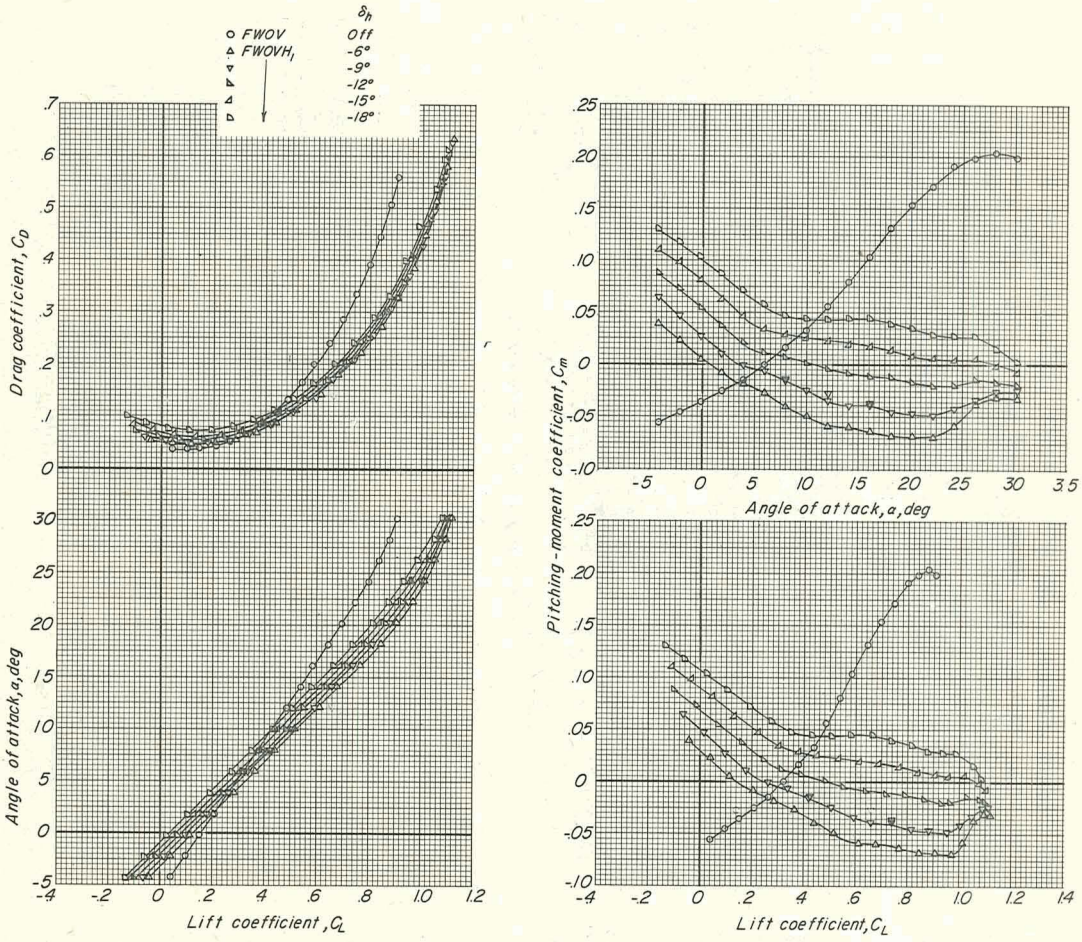

(b) $\delta_f = 30^\circ$; $\delta_n = 0^\circ$.

Figure 9.- Continued.

CONFIDENTIAL

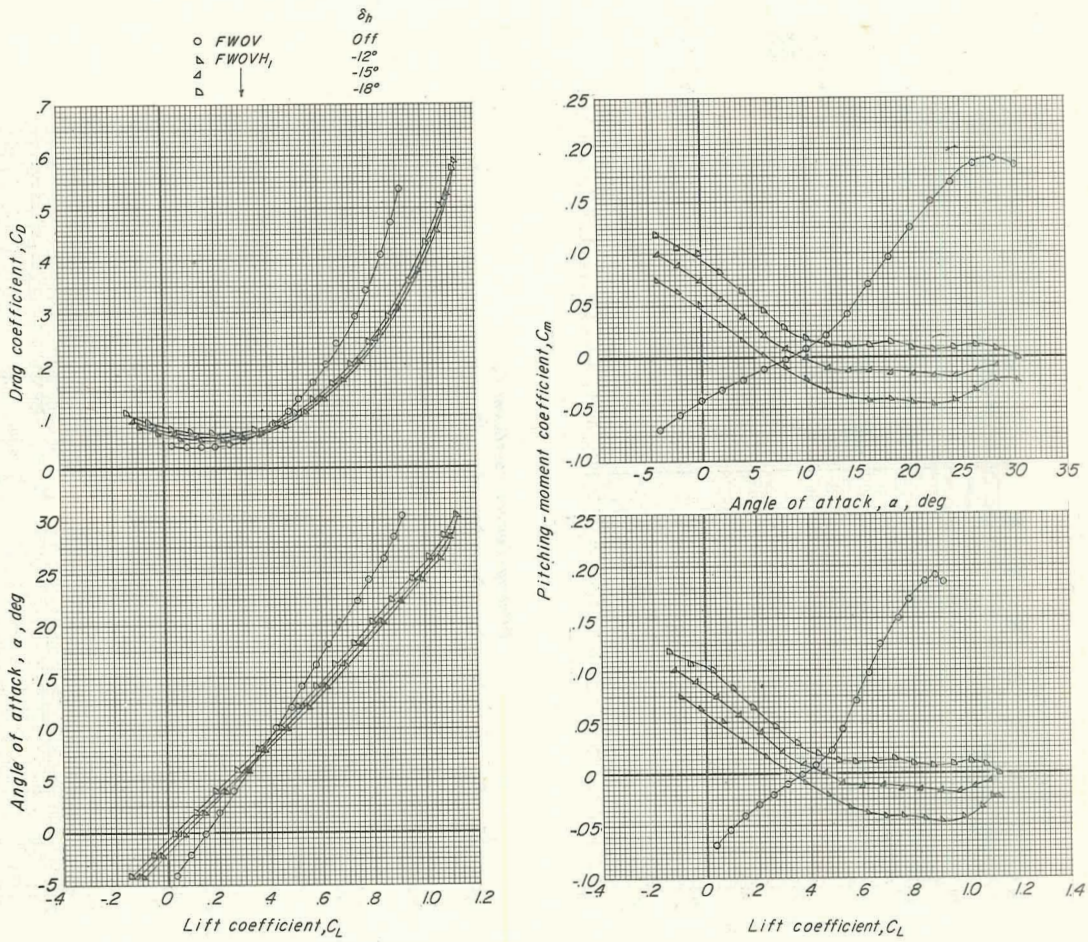

(c) $\delta_f = 30°$; $\delta_n = -15°$.

Figure 9.- Concluded.

CONFIDENTIAL

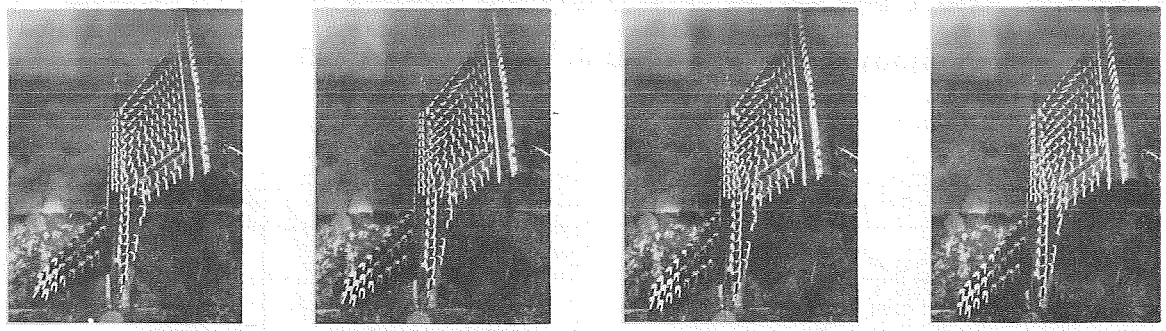

$\alpha = 5.83°$ $C_L = .06$ $\alpha = 7.87°$ $C_L = .14$ $\alpha = 9.91°$ $C_L = .22$ $\alpha = 11.96°$ $C_L = .31$

(a) $\delta_f = 0°$; $\delta_n = 0°$.

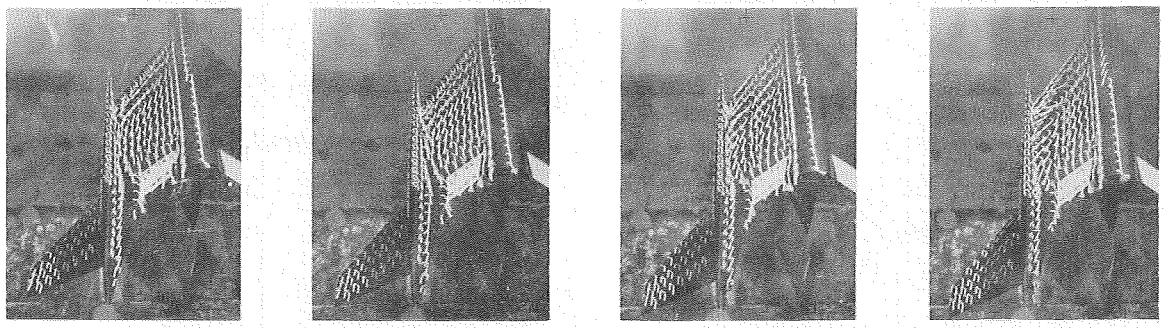

$\alpha = 5.94°$ $C_L = .27$ $\alpha = 7.98°$ $C_L = .35$ $\alpha = 10.02°$ $C_L = .43$ $\alpha = 12.06°$ $C_L = .51$

(b) $\delta_f = 30°$; $\delta_n = -15°$.

L-60-2490

Figure 10.- Photographs of wing-surface tufts showing effects of flap deflection on the flow over the upper surface of the wing. $\delta_h = -18°$.

CONFIDENTIAL

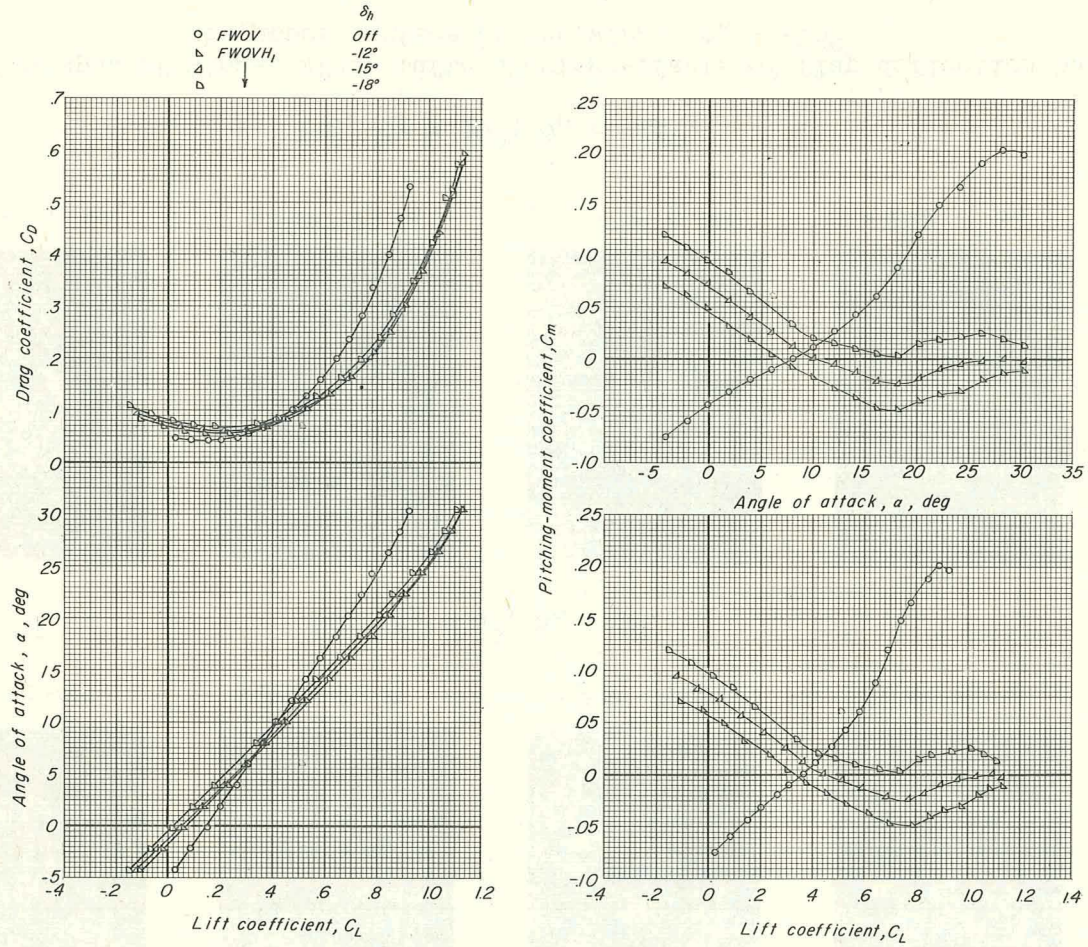

(a) Longitudinal aerodynamic characteristics.

Figure 11.- Longitudinal aerodynamic characteristics of the model with 1/3-semispan leading-edge chord extensions on the model. $\delta_f = 30°$; $\delta_n = -15°$.

CONFIDENTIAL

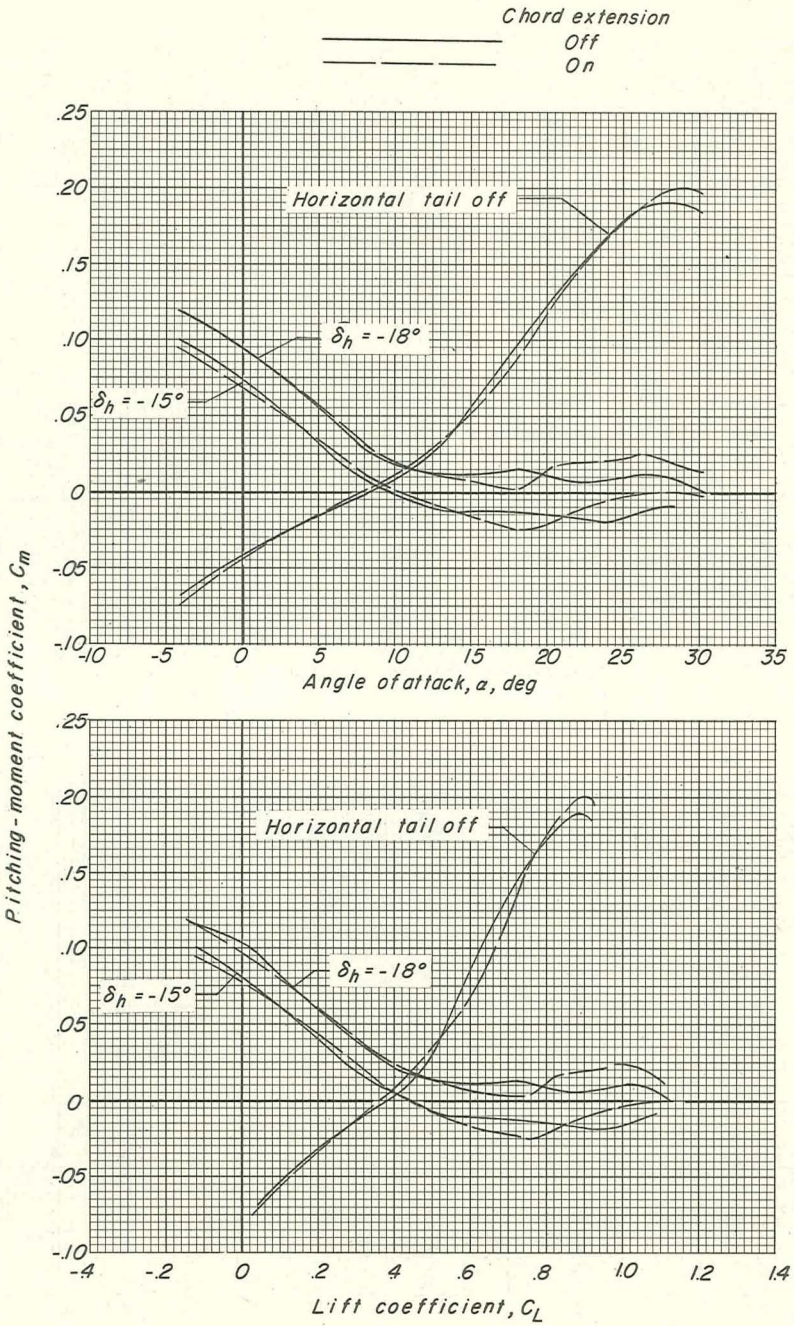

(b) Effect of chord extensions on pitching-moment characteristics.

Figure 11.- Concluded.

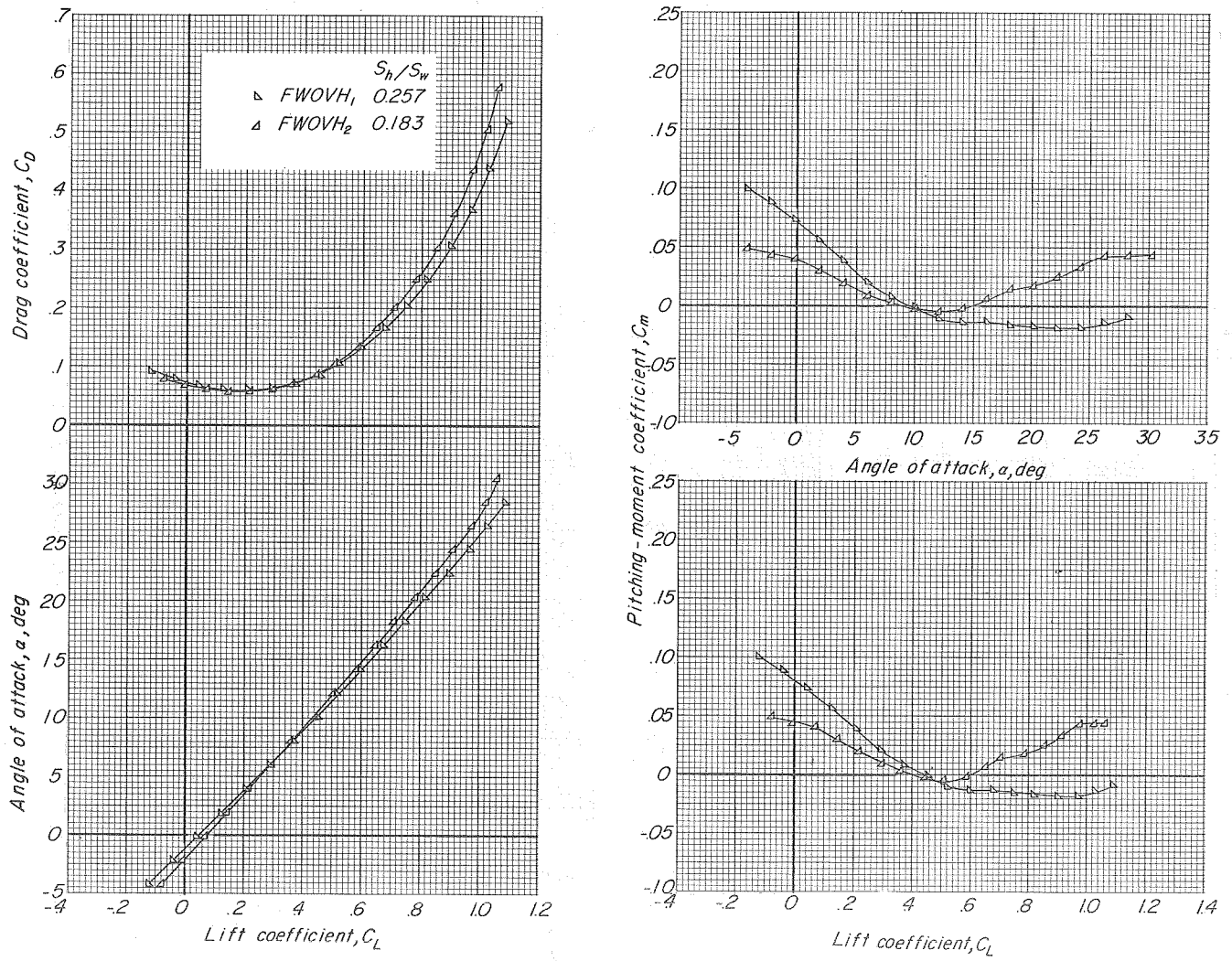

Figure 12.- Effect of horizontal-tail area on the longitudinal aerodynamic characteristics of the model. $\delta_f = 30°$; $\delta_n = -15°$; $\delta_h = -15°$.

CONFIDENTIAL

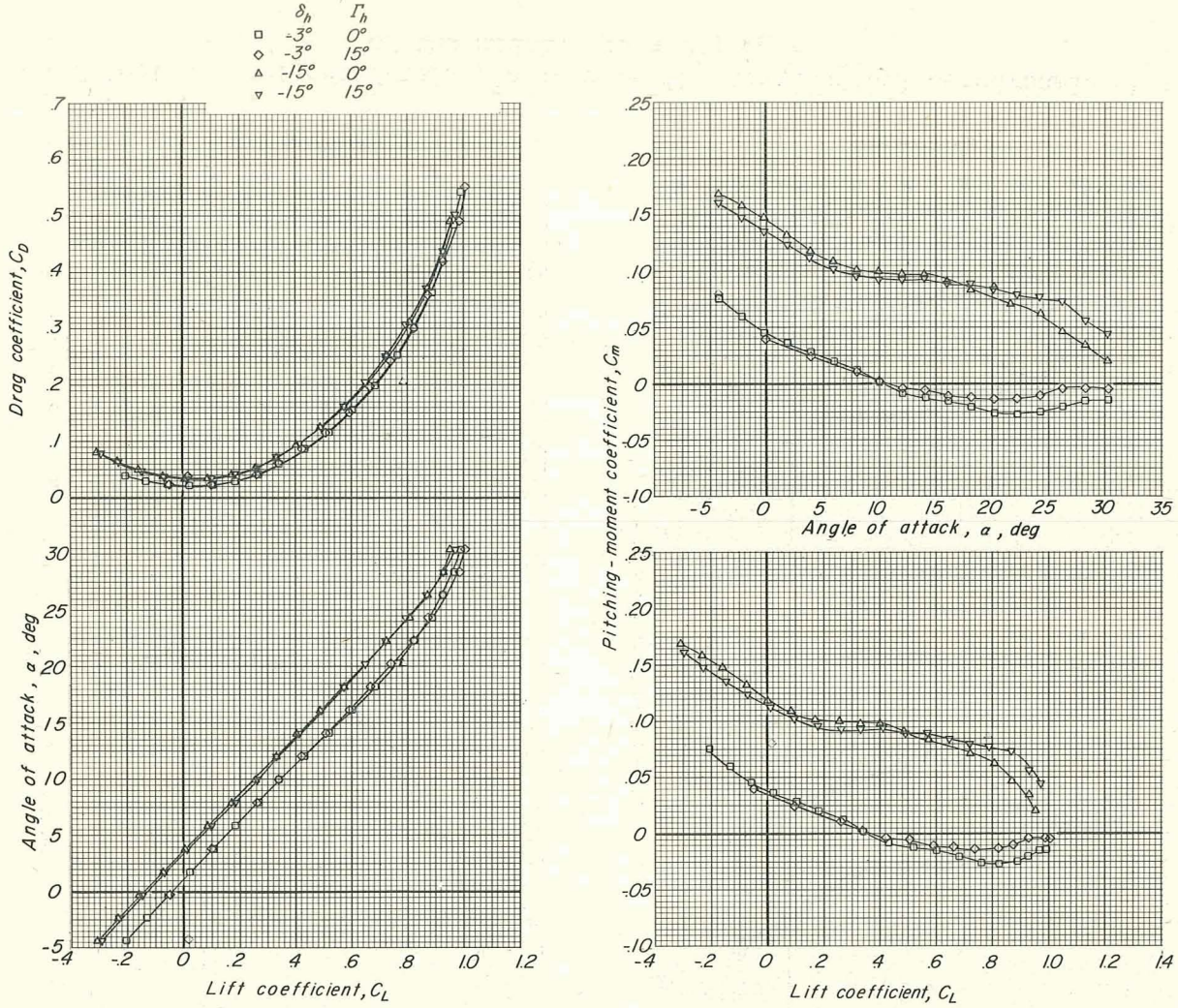

Figure 13.- Effect of horizontal-tail dihedral on the longitudinal aerodynamic characteristics of the model. $FWOVH_1$; $\delta_f = 0^\circ$; $\delta_n = 0^\circ$.

CONFIDENTIAL

CONFIDENTIAL

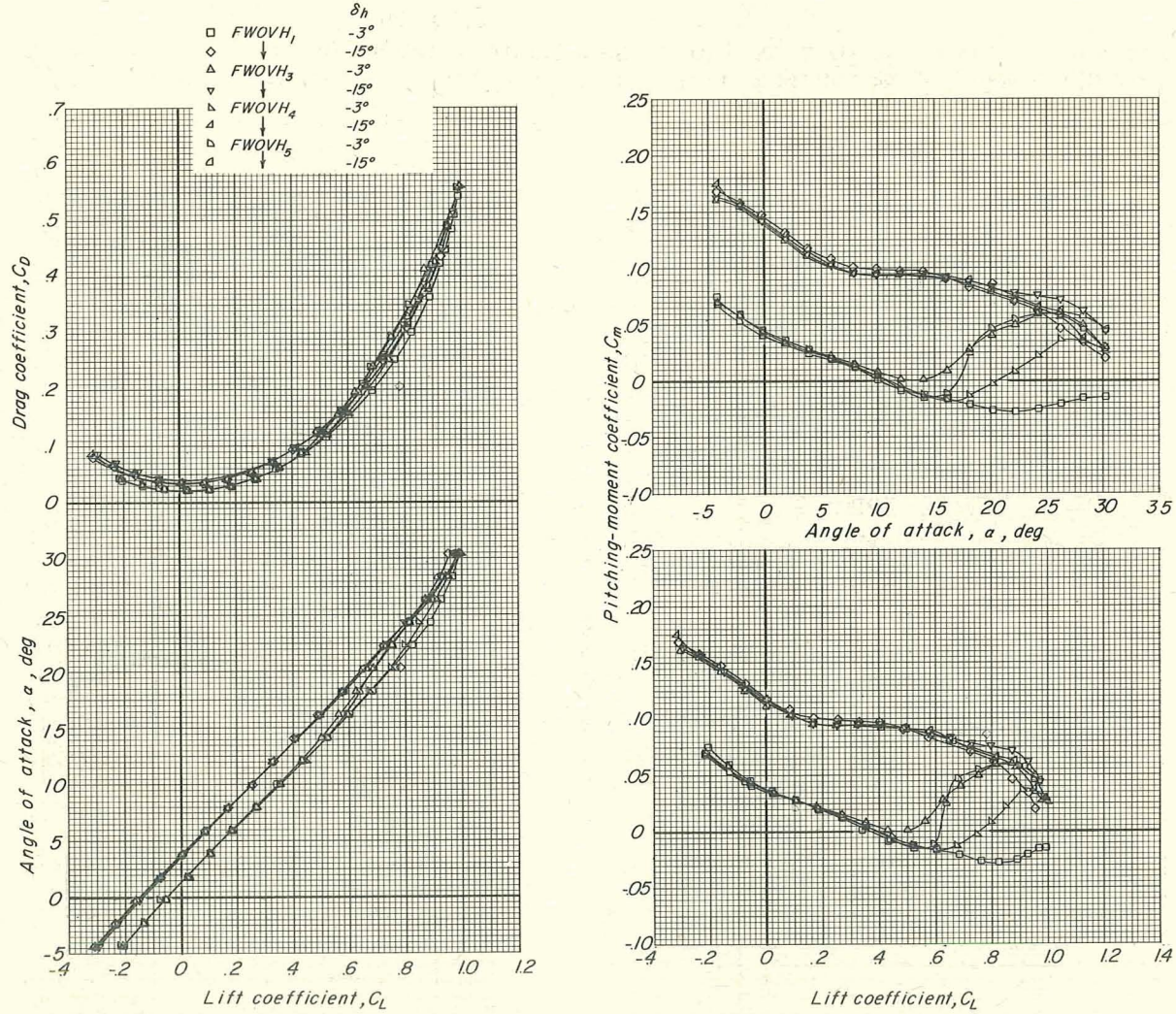

Figure 14.- Effect of horizontal-tail planform on the longitudinal aerodynamic characteristics of the model. $\delta_f = 0^\circ$; $\delta_n = 0^\circ$.

CONFIDENTIAL

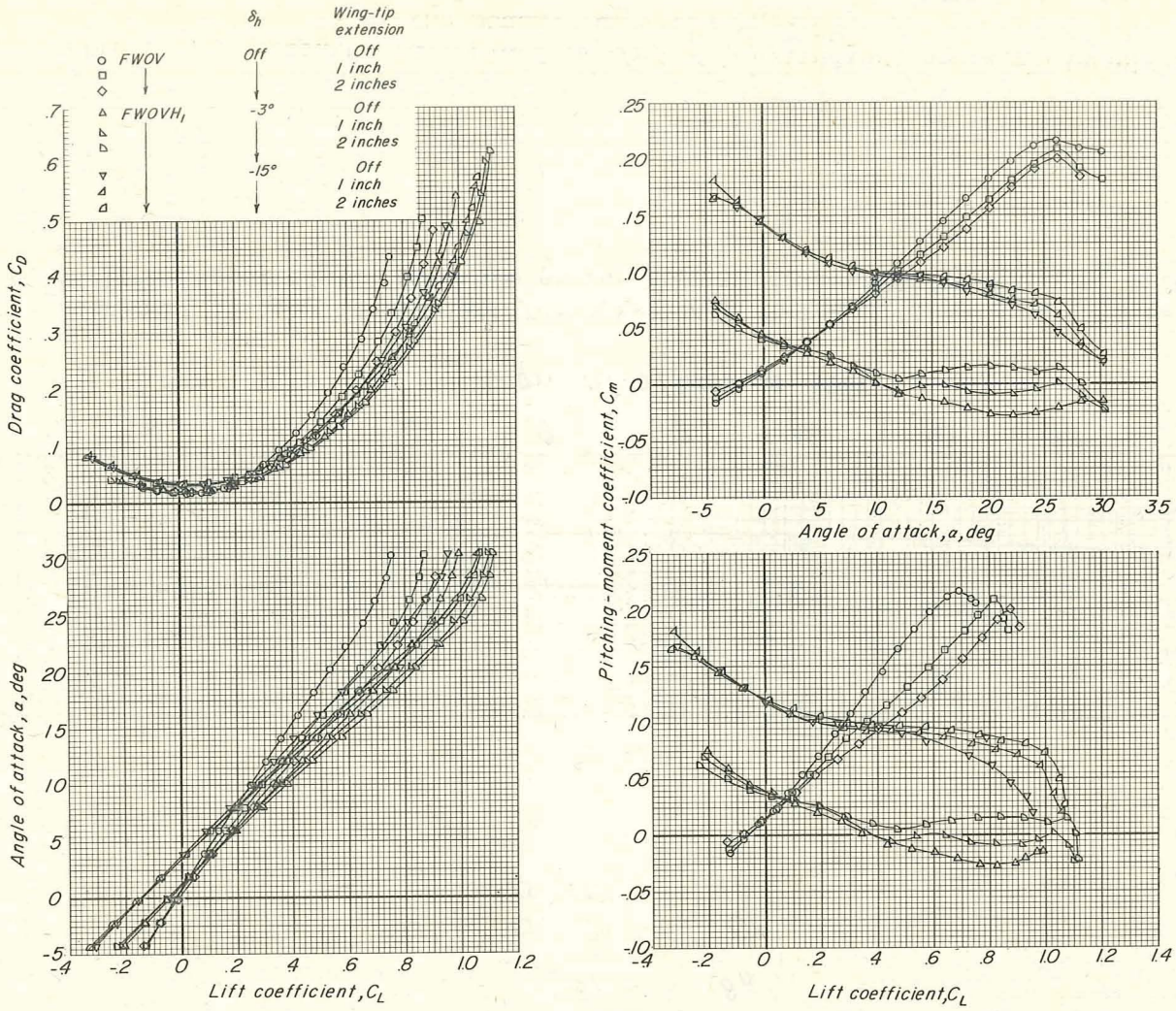

Figure 15.- Effect of wing-tip span extensions on the longitudinal aerodynamic characteristics of the model. $\delta_f = 0^\circ$; $\delta_n = 0^\circ$.

CONFIDENTIAL

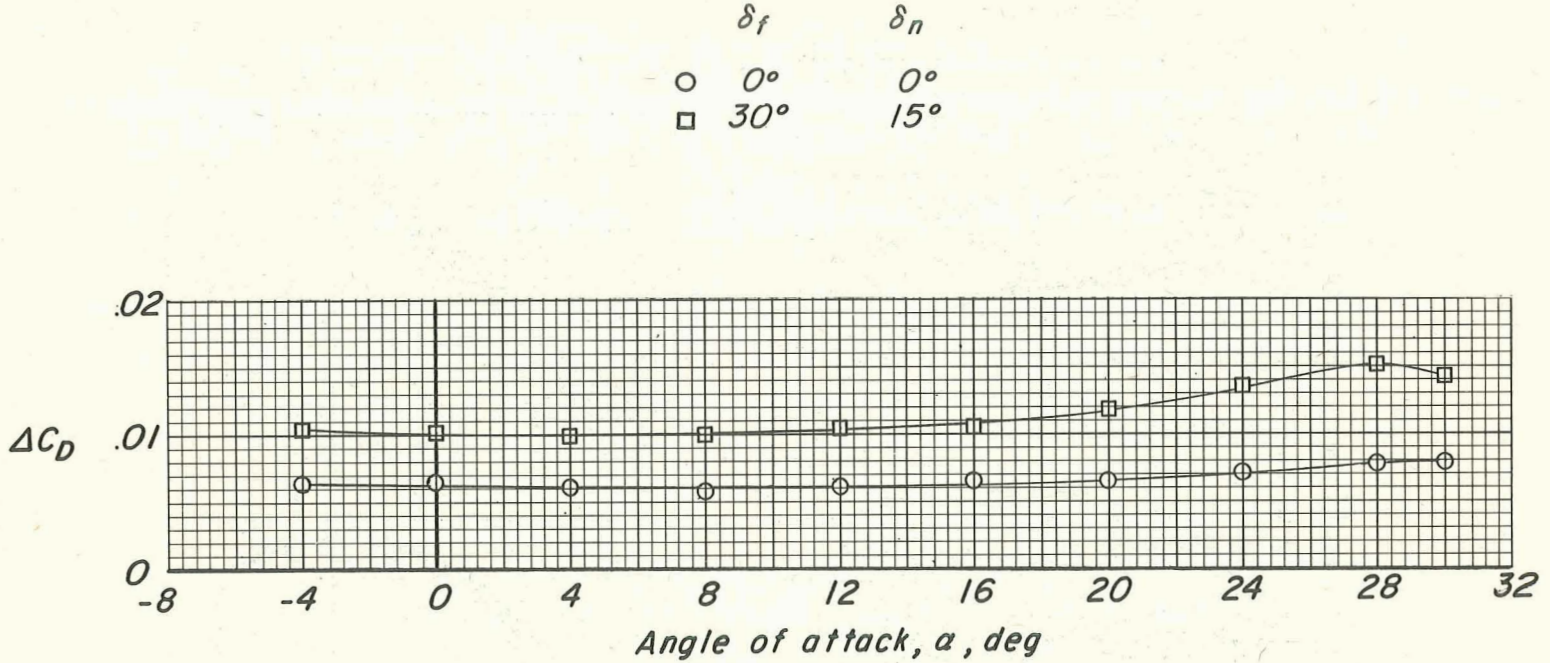

Figure 16.- Increment in drag coefficient for correcting the model drag coefficients to conditions of free-stream static pressure at the base of the model. $FWOVH_1$; $\delta_h = -9^\circ$.

CONFIDENTIAL

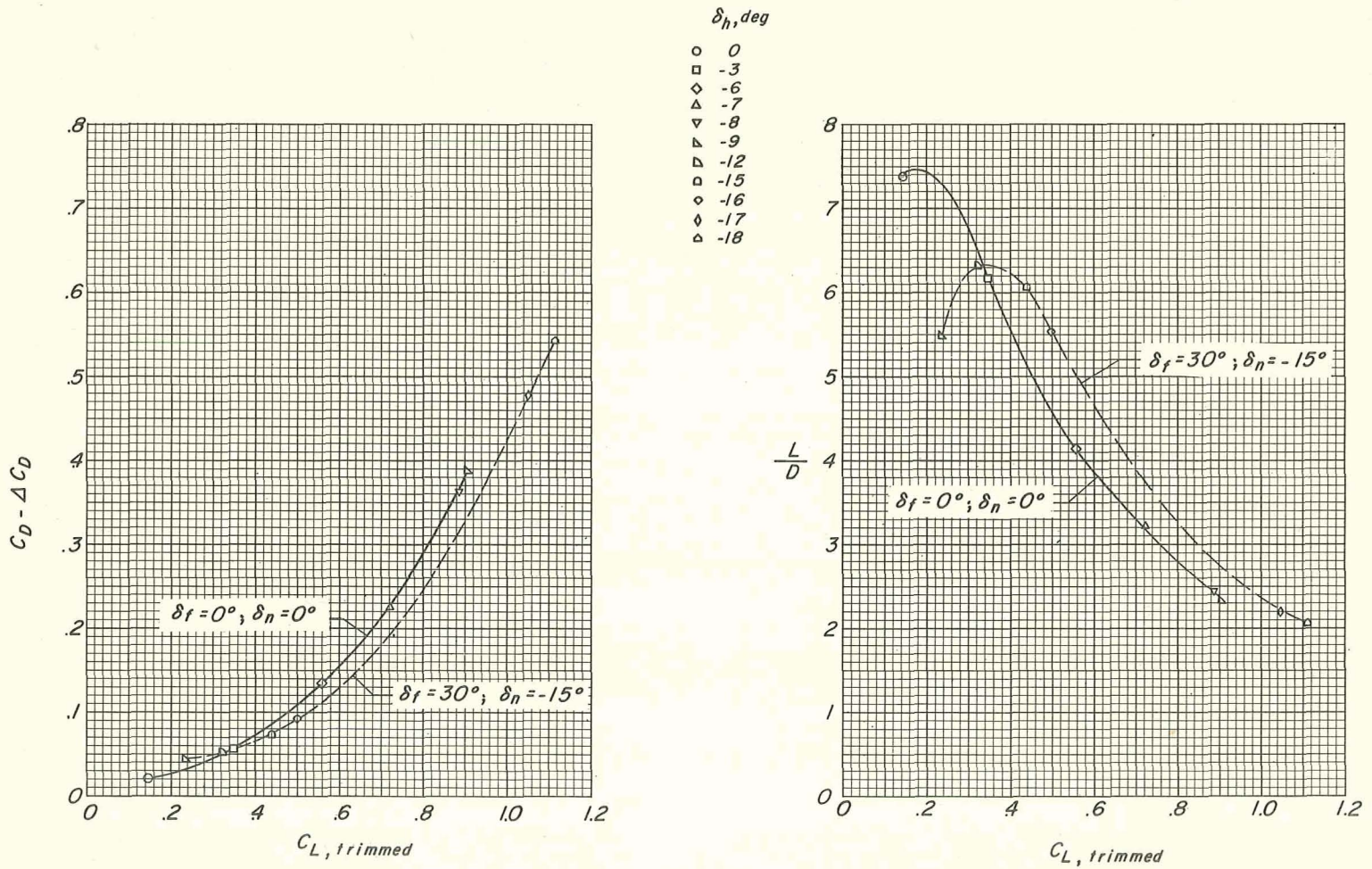

Figure 17.- Effect of flap deflection on the drag polars and lift-drag ratios of the model for trimmed conditions. Drag coefficients have been corrected for base pressure.

CONFIDENTIAL

CONFIDENTIAL

CONFIDENTIAL